

Reionization and its sources

Anirban Chakraborty^a and Tirthankar Roy Choudhury^a

^aNational Centre for Radio Astrophysics, Tata Institute of Fundamental Research, Pune University Campus, Ganeshkhind, Pune 411007, India

© 20xx Elsevier Ltd. All rights reserved.

Chapter Article tagline: update of previous edition,, reprint..

Abstract

Reionization represents an important phase in the history of our Universe when ultraviolet radiation from the first luminous sources, primarily stars and accreting black holes, ionized the neutral hydrogen atoms in the intergalactic medium (IGM). This process follows the “Dark Ages”, a period with no luminous sources, and is initiated by the formation of the first sources, marking the “Cosmic Dawn”. Reionization proceeds through multiple stages: initially, ionized bubbles form around galaxies, then expand and overlap across the IGM, culminating in a fully ionized state, with neutral hydrogen remaining only in dense regions. Understanding reionization involves a diverse range of physical concepts, from large-scale structure formation and star formation to radiation propagation through the IGM. Observationally, reionization can be explored using the cosmic microwave background (CMB), Lyman- α absorption, high-redshift galaxy surveys, and emerging 21 cm experiments, which together offer invaluable insights into this transformative epoch.

Keywords Reionization, Intergalactic Medium, First Stars, Primordial Galaxies, Early Universe, Cosmology, Large-scale structure of the universe, Lyman alpha forest, Cosmic microwave background radiation

Nomenclature

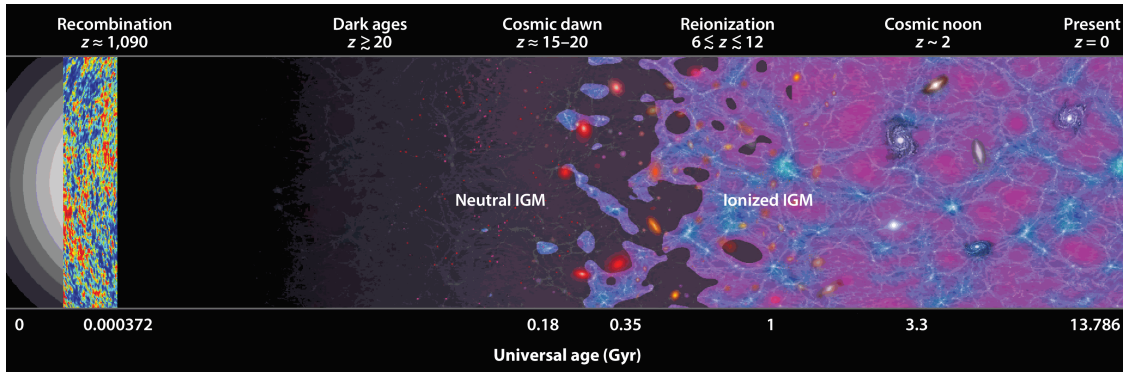
CMB	Cosmic Microwave Background
DM	Dark Matter
CDM	Cold Dark Matter
IGM	Intergalactic medium
UV	Ultraviolet
EoR	Epoch of Reionization
IMF	Initial Mass Function
ISM	Interstellar medium
CGM	Circumgalactic medium
AGN	Active Galactic Nuclei
kSZ	kinetic Sunyaev-Zel'dovich
GP	Gunn-Peterson
HST	Hubble Space Telescope
JWST	James Webb Space Telescope
LAEs	Lyman Alpha Emitters
LBGs	Lyman Break Galaxies
SKA	Square Kilometre Array
DM	Dispersion Measure
FRBs	Fast Radio Bursts

1 Learning Objectives

By the end of this chapter, the reader is expected to understand:

- The meaning of cosmic reionization and its significance in the evolution of the Universe.
- How reionization proceeds, both qualitatively and quantitatively, with time.
- The different kinds of ionizing sources that may have been responsible for driving reionization.
- How reionization can be studied through various observations such as the cosmic microwave background (CMB), Lyman- α absorption, high-redshift galaxy surveys, and upcoming 21 cm experiments.

2 Reionization and its sources



Robertson BE, 2022
Annu. Rev. Astron. Astrophys. 60:121-58

Fig. 1: An illustration highlighting the various milestones in the evolutionary history of our Universe, since the Big Bang. The figure shows the evolution of the ionization state of the IGM due to ionizing radiation from the earliest generation of luminous sources, alongside the corresponding evolution in their abundances. Image Credits: Robertson (2022)

2 Introduction

Our understanding of the Universe’s evolutionary history is based on the foundations of the standard hot Big Bang model, which has received considerable observational support over time. According to this paradigm, the Universe was extremely hot and dense in its initial moments, with photons existing in thermal equilibrium with matter. As the Universe expanded, its temperature and density gradually dropped. Around three minutes after the Big Bang, nuclei of elements heavier than hydrogen (mainly helium and lithium) formed through a process called nucleosynthesis. About 380,000 years later, the temperature decreased further, allowing hydrogen, helium, and lithium nuclei to capture electrons and form neutral atoms. With the formation of the first atoms, photons were no longer scattered by free electrons in the plasma and could travel freely through the Universe. These photons are observed today as the cosmic microwave background (CMB) radiation, providing the earliest possible view of the Universe. Soon after the recombination epoch, the Universe entered a phase called the “Dark Ages”, where no significant radiation sources existed, and hydrogen remained largely neutral. During this period, small perturbations in the matter density present at the time of recombination began to grow due to gravitational instability. In this process, slightly overdense regions accreted matter from surrounding underdense regions due to their self-gravity, becoming increasingly overdense. As these overdense regions continued to accrete more and more matter, they expanded at an increasingly slower pace compared to the background Universe, ultimately breaking away from the background expansion and collapsing under their own gravity. During this gravitational collapse, the infalling matter particles interacted gravitationally amongst themselves and exchanged energies, eventually reaching a state of virial equilibrium. This marked the formation of gravitationally bound structures known as “dark matter haloes”, as the matter component of the Universe is dominated by the dark matter (DM). In the context of the cold dark matter (CDM) model of structure formation, these newly formed DM haloes continue to evolve, growing in mass and size either by accreting material from their surroundings or by merging with other haloes.

These collapsed dark matter-dominated haloes form potential wells, into which the baryons passively fall. It should, however, be kept in mind that most of the baryons at high redshifts do not reside within these collapsed DM haloes, they rather reside as diffuse gas within the intergalactic space which is known as the intergalactic medium (IGM). The baryonic gas, when attracted into the dark matter potential well, acquires kinetic energy and is heated up to the virial temperature of the halo via shocks. Further evolution can only take place if this shock-heated gas can somehow cool. If the mass of the halo is sufficiently high (i.e., the potential well is deep enough), the gas will be able to dissipate its internal energy via atomic or molecular transitions and fragment within the halo. This produces conditions appropriate for gas to condense and form stars (and eventually, galaxies), thereby marking the end of the era of the “Dark Ages” and the onset of “Cosmic Dawn”. Once these earliest luminous sources (i.e., stars inside galaxies) form, they produce copious amounts of ultraviolet (UV) radiation through thermonuclear reactions in their cores. In addition to galaxies, a population of early black holes may have also contributed to this UV radiation. Some of this radiation escapes out of these systems, carrying photons with energies of ≥ 13.6 eV that ionize the surrounding neutral hydrogen atoms, initiating the “Epoch of Reionization” (EoR). As more luminous sources formed, the individual ionized bubbles localized around the earliest sources began to overlap, gradually expanding to fill larger volumes of the Universe with ionized gas. This process finally concluded around a billion years after the Big Bang, marking a significant phase transition in the ionization state of hydrogen atoms in the IGM. By the end of reionization, the hydrogen in the Universe was almost fully ionized (see Figure 1 for an illustration of the timeline). The sources, primarily stars, that ionize hydrogen are also capable of singly ionizing helium ($\text{HeI} \rightarrow \text{HeII}$) through photons with energies of ≥ 24.6 eV and the first reionization of helium is thus believed to be roughly contemporaneous with that of hydrogen. However, the removal of the second electron from helium (known as HeII reionization) requires photons with even higher energies (≥ 54.4 eV), which are generated by more powerful sources, such as accreting black holes (commonly referred to as quasars), and occurs at a much later time. In this article, we will concentrate mostly on hydrogen reionization by the first luminous sources.

From an observational standpoint, the era of cosmic reionization is a largely unexplored phase of the Universe. It serves as a crucial

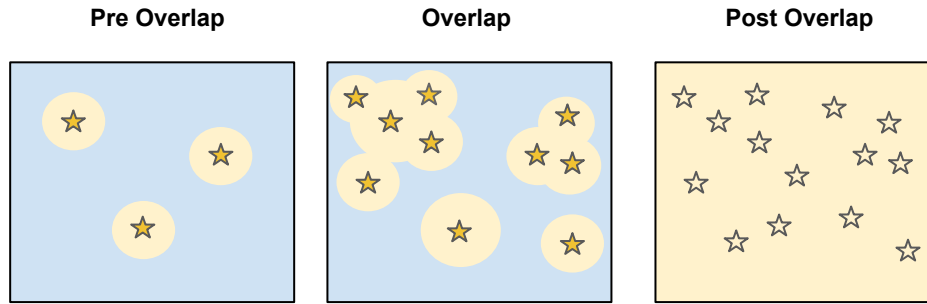


Fig. 2: A cartoon illustration depicting the different phases of reionization. Initially, ionized bubbles form around individual sources (represented by star symbols here), then expand and merge with other surrounding bubbles until the entire IGM is completely ionized, with neutral hydrogen remaining only in dense regions (not shown in the figure).

link between the early Universe, which we study through the CMB, and the late Universe, which is well understood through observations of galaxies, clusters, quasars, and other astronomical sources. Over the last few years, the availability of high-quality datasets obtained from various cutting-edge telescopes that probe the earliest epochs of our Universe has provided a fresh impetus to the study of cosmic reionization and the first stars. Moreover, understanding cosmic reionization is essential for studying how structures in the Universe formed and evolved since it not only results from the formation of the first luminous sources but also influences the formation and evolution of structures at later epochs. For instance, during reionization, ionizing photons not only ionized neutral atoms but also heated the IGM through transfer of the excess energy carried by the free electrons. This additional heating in ionized regions affects the subsequent formation of stars by either expelling gas or preventing gas from being efficiently cooled, particularly in low-mass haloes. The details of the reionization process, among other factors, depend on the properties of the ionizing sources. Therefore, reionization studies provide a complementary approach to understanding the earliest generation of luminous sources through their impact on the IGM — particularly those too faint to be detected directly, even with next-generation telescopes.

In this chapter, we present an overview of our current understanding of cosmic reionization and its probable sources and highlight how the Epoch of Reionization can be probed through a wide variety of observations. The chapter is organized as follows: In Section 3, we briefly describe the stages of reionization and how the same can be studied using theoretical models. This is followed by a discussion of the potential sources of ionizing radiation that may have contributed to cosmic reionization in Section 4. We discuss the different observational probes that can shed light on the properties of the ionizing sources and the missing details about reionization in Section 5.

3 The stages of hydrogen reionization

The reionization of hydrogen occurs in several stages, as shown in Figure 2, starting with the “pre-overlap” phase. In this initial stage, individual ionizing sources light up and begin ionizing the surrounding medium, which is predominantly composed of hydrogen. This process results in the formation of a region of photoionized gas, known as an HII region, around each source. These cosmological HII regions gradually grow as ionizing radiation propagates deeper into the neutral intergalactic medium. Since the first ionizing sources are thought to form in high-density regions of the Universe, their ionizing fronts must navigate through these dense environments, where the recombination rates are also typically high. Beyond these dense regions, however, the ionizing fronts spread more easily through the low-density voids of the Universe. As these HII regions expand, they leave behind some clumps of neutral, high-density gas, which, owing to their higher recombination rates, require more ionizing photons to become ionized than are available at this stage. During this time, the IGM exists in the form of a two-phase medium with the highly ionized (HII) regions separated from neutral regions by ionization fronts. Although the intensity of ionizing radiation is initially low, it gradually increases over time during the pre-overlap stage.

Because the first collapsed objects tend to form in the densest regions of the universe, their distribution is not a direct tracer of the overall matter distribution but is instead amplified in the highest-density peaks. As a result, the earliest luminous sources are strongly clustered. Consequently, reionization quickly progresses into its second stage, known as the “overlap” phase. During this phase, neighboring HII regions begin to coalesce, and the ionizing background rapidly increases as an increasing number of newly formed sources power each HII region. Therefore, the ionization fronts can now expand into even regions with high gas density that had previously remained neutral. By the end of this phase, all low-density regions of the IGM as well as some of the high-density regions that were located close to the ionizing

4 Reionization and its sources

sources are completely ionized. A small fraction of neutral gas however remains confined within dense structures that were located far from any ionizing source. As more and more ionizing sources continue to form, these high-density regions are also expected to get gradually ionized, leading to an increasingly uniform ionizing background. This final stage, known as the “post-overlap” phase, continues indefinitely - in fact, collapsed objects such as galaxies still have neutral gas trapped inside them in the local Universe.

From the above discussion, it is evident that cosmic reionization progresses at different rates in different regions of the Universe. On average, regions with a higher concentration of ionizing sources undergo reionization more rapidly compared to those where such sources are scarce. This overall description of reionization, where the process begins in high-density regions hosting ionizing sources and extends outward to low-density voids, is commonly referred to as “inside-out” reionization. While this holds true during the initial stages of reionization, there is a shift in the pattern of reionization when it approaches the later stages of the overlap phase. In its final stages, the high recombination rates in dense regions dominate the process and reionization penetrates deep into underdense regions before gradually evaporating the denser neutral regions. This results in a more “outside-in” progression, with low-density regions getting ionized earlier than the high-density regions. In this regard, reionization can be viewed as a process that essentially evolves in an “inside-out-in” manner. Understanding the various stages of reionization involves solving complex, non-linear physics, which is feasible only through detailed radiative transfer simulations. These simulations aim to model the transport of radiation through the cosmological matter field while simultaneously tracking the thermal and ionization states of the gas. Given the broad range of spatial and temporal scales involved, such studies are computationally intensive (Gnedin and Madau, 2022). Recently, efforts have been made to study reionization using approximate yet computationally efficient simulations known as semi-numerical simulations. These simulations replace detailed radiative transfer with a simplified photon-counting algorithm and typically employ coarser resolutions than full simulations (Furlanetto et al., 2004; Mesinger and Furlanetto, 2007; Choudhury et al., 2009; Santos et al., 2010; Mesinger et al., 2011; Choudhury and Paranjape, 2018; Hutter, 2018; Mondal et al., 2021; Schaeffer et al., 2023).

The progress of reionization can be approximated using an evolution equation for the globally averaged ionization fraction (Madau et al., 1999)

$$\frac{dQ_{\text{HII}}(t)}{dt} = \frac{1}{\bar{n}_H} \frac{dn_{\text{ion}}(t)}{dt} - Q_{\text{HII}}(t) \chi_{\text{He}}(t) \bar{n}_H a^{-3}(t) C(t) \alpha_R(T), \quad (1)$$

where Q_{HII} is the fraction of volume ionized, $dn_{\text{ion}}(t)/dt$ denotes the number density of ionizing photons produced by the sources and available for reionization in the IGM per unit time per unit comoving volume, \bar{n}_H is the present-day mean comoving number density of hydrogen, $a(t)$ is the cosmological scale factor, $\alpha_R(T)$ is the recombination rate coefficient which depends on the temperature T of the medium, $\chi_{\text{He}}(t)$ denotes the number of free electrons per hydrogen atom (which includes the excess contribution from helium, depending on its ionization state) and $C(t)$ is the clumping factor that accounts for enhanced recombinations in an inhomogeneously ionized IGM. The above equation can be interpreted as follows: the total number of ionizing photons produced (the first term on the right-hand side) is used either to ionize regions that were previously neutral (the term on the left-hand side) or to re-ionize recombined atoms within already ionized regions (the second term on the right-hand side). This equation can be readily solved to obtain the reionization history $Q_{\text{HII}}(t)$ when supplemented with a model for the emissivity of ionizing photons $dn_{\text{ion}}(t)/dt$ and clumping $C(t)$. Despite the simplifying assumptions in the above equation (e.g., ignoring density dependence in the growth of ionized regions and assuming ionizing photons are almost immediately absorbed by the diffuse IGM), it is widely used to model the progression and history of reionization, and also fares well when compared with more detailed radiative transfer simulations.

Before proceeding further, let us look at the reionization histories for a simplistic model where the comoving number density of ionizing photons available for reionization is parameterized as $n_{\text{ion}}(t) = \bar{n}_H \zeta(t) f_{\text{coll}}(M_{\text{min}}, t)$. Here, $\zeta(t)$ denotes the number of ionizing photons injected into the IGM per hydrogen atom inside collapsed objects, while $f_{\text{coll}}(M_{\text{min}}, t)$ denotes the fraction of mass contained in collapsed objects of mass $M \geq M_{\text{min}}$ at a given cosmic epoch t . In general, the ionization efficiency parameter ζ encapsulates information about several other poorly understood astrophysical processes such as the star-forming efficiency within the collapsed structure, the number of ionizing photons produced per unit stellar mass, and the escape probability of these photons. For simplicity, we assume that the two unknown parameters ζ and C appearing in equation (1) do not evolve with time. Therefore, under these assumptions, we can rewrite equation (1) as

$$\frac{dQ_{\text{HII}}(t)}{dt} = \zeta \frac{df_{\text{coll}}(M_{\text{min}}, t)}{dt} - Q_{\text{HII}}(t) \chi_{\text{He}}(t) \bar{n}_H a^{-3}(t) C \alpha_R(T), \quad (2)$$

The left-hand panel of Figure 3 shows the reionization histories obtained by numerically solving equation (2) for representative values of ζ and C . Here, we fix the minimum mass of haloes M_{min} contributing to the ionizing photon budget to be $10^8 M_{\odot}$, appropriate for atomically cooled haloes (to be discussed in the next section). From the figure, one can see that when the efficiency of ionizing photon production is increased (i.e., the value of ζ becomes larger, keeping C unchanged), reionization progresses faster and completes earlier due to the availability of a higher number of ionizing photons. On the other hand, if the IGM is assumed to be excessively clumpy (i.e., the value of C becomes larger, keeping ζ unchanged), the progress of reionization is slowed down since the recombination rate gets enhanced due to increased clumpiness and hence more ionizing photons are now consumed in ionizing the recombined atoms. We show the effect of varying the value of M_{min} (keeping ζ and C unchanged) in the right-hand panel of Figure 3. Raising the value of M_{min} leads to a delayed onset of reionization, since larger haloes form comparatively later in the Universe due to the hierarchical nature of structure formation.

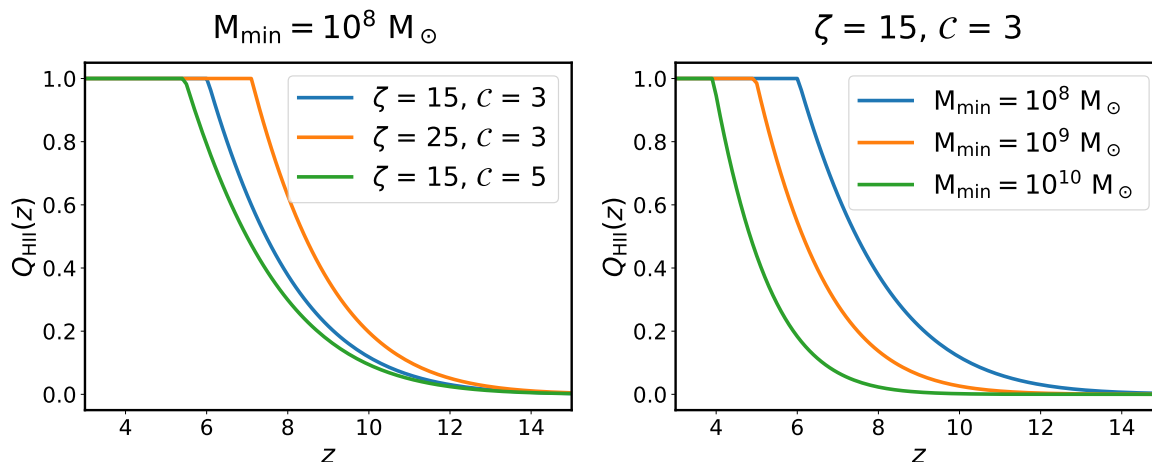


Fig. 3: The evolution of the ionized volume fraction Q_{HII} of the Universe as a function of redshift z corresponding to some representative values of the ionization efficiency parameter ζ and clumping factor C (*left-hand panel*) and the minimum mass M_{min} of haloes capable of producing ionizing photons (*right-hand panel*). It has been assumed that none of these three parameters vary over time.

4 Sources responsible for cosmic reionization

4.1 Star-forming galaxies

The stars in the earliest galaxies are considered to be the most promising sources of ionizing UV photons, largely due to their high abundance during this era. Understanding the key factors that influence the formation of stars and the production of ionizing radiation from these systems at such early epochs is therefore of great importance. As mentioned earlier, these stars form within dark matter haloes massive enough to attract the surrounding baryonic material (mainly, gas). However, for this accreted gas to be able to form stars, it must first undergo rapid gravitational collapse — i.e., the force of gravity must exceed its internal pressure. But, this alone is not sufficient, since the temperature of the gas rises rapidly during contraction, leading to an increase in its internal pressure that resists further gravitational collapse. Eventually, the gas, after being shock-heated to temperatures close to the halo’s virial temperature, settles into an equilibrium configuration where it is supported against gravity by its thermal pressure. Without any other dissipative mechanisms, the gas would remain in this low-density, hot state indefinitely, preventing star formation. Therefore, a second key requirement is that the gas must cool and condense into dense molecular clouds, where star formation can finally occur.

In principle, gaseous matter can cool down by losing its internal energy through various atomic processes, such as collisionally-excited emission and different types of continuum radiation, including bremsstrahlung, recombination, and collisional ionization. Such cooling is effective only when it takes place much faster than the free-fall timescale of the system. However, at high redshifts, where the gas is primarily composed of hydrogen and helium atoms, the dominant cooling process is the collisional excitation of atoms and subsequent radiative de-excitation. In this case, the atoms get excited to a higher energy level because of a collision with another atom and then return to the lower state by emitting photons. If these photons are able to escape the halo, carrying away energy, the system will cool down. However, below a temperature of 10^4 K (corresponding to a halo mass $M \sim 10^8 M_{\odot}$), cooling via atomic transitions is not very effective because collisions among the atoms do not have sufficient energy to excite the atoms. In the absence of heavy elements, cooling at low temperatures ($T \leq 10^4$ K) is primarily facilitated by molecules like hydrogen (H_2), whose rotational and vibrational levels can be excited by low-energy electrons. In these pristine conditions, the formation of H_2 , catalyzed by free electrons left over from the epoch of recombination, enables efficient cooling even in small haloes (commonly known as minihaloes) with masses around $M \sim 10^6 M_{\odot}$.

Tracking the precise cooling mechanisms, followed by gas condensation and fragmentation that ultimately lead to star formation, is a highly complex process. Nevertheless, we outline the key physical processes essential for star formation within collapsed haloes. Gas cooling leads to a drop in pressure, which, in turn, lowers the critical mass required for gravity and pressure to balance. This leads to fragmentation of the gas in the halo, where the gas clouds break up into even smaller and smaller clumps. However, this fragmentation process eventually stops when the gas becomes dense and optically thick, at which point the cooling timescale exceeds the free-fall timescale. The masses of the stars formed depend on when and how the fragmentation stops. The distribution of the stellar masses m_* in a newly formed stellar population is usually characterized by the stellar initial mass function (IMF), defined as the relative number of stars born with mass in a given range. At very high redshifts, when the cooling was not very efficient in the absence of metals, the fragmentation stopped early and the stars formed tended to have much higher mass leading to a “top-heavy” IMF. These stars, formed from pristine gas, are expected to be extremely metal-poor and known as the *Population III* (*Pop III*) stars. Due to their chemical composition, Pop III stars could only generate energy through nuclear fusion via the proton-proton (p-p) cycle, as they lacked the heavier elements required to fuel the more efficient CNO cycle. As a result, these stars were incredibly hot and possessed a very hard emission spectrum, producing far more energetic photons than

the stars we see today, making Pop III stars highly efficient sources of ionizing photons in the early Universe.

Once these first stars begin to form, the energy released by them in the form of radiation or mechanical outflows can significantly impact the formation of subsequent stars through various “feedback” effects. For instance, molecular cooling within minihaloes is extremely short-lived because hydrogen molecules are highly susceptible to dissociation by UV photons with energies between 11.26 and 13.6 eV, which are emitted by the very first stars. As molecular hydrogen is gradually depleted, star formation in the smallest minihaloes begins to be suppressed. Ultimately, this Lyman-Werner radiation background becomes so intense that Pop III star formation is entirely switched off in pristine minihaloes. Further episodes of star formation will then have to wait until the haloes grow large enough, attaining masses $\geq 10^8 M_\odot$ so that the gas temperature crosses the threshold ($> 10^4$ K) for atomic cooling to become efficient.

Additionally, given that Pop III stars are extremely massive, they have significantly shorter lifetimes (approximately 10^6 years), and end their lives in various types of supernova explosions depending on their initial mass. Among these, the most intriguing are the Pop III stars with masses in the range of 100 - 260 M_\odot , which explode as Pair Instability Supernovae (PISN). These supernovae have exceptionally high metal yields, converting roughly half of their mass into heavy elements. Such energetic explosions, along with powerful stellar winds during the late stages of stellar evolution, enrich the surrounding gas with metals produced inside the cores of the first stars. As a consequence, species such as singly ionized carbon (CII) and neutral oxygen (OI) then help in increasing the cooling rate through excitation of their atomic fine-structure levels, allowing the gas to reach even lower temperatures and fragment into stars with significantly lower masses. This marks the onset of the more “conventional” metal-enriched mode of star formation in haloes, leading to the formation of the second generation of stars, known as *Population II (Pop II)* stars, whose IMF is dominated by low-mass stars and have a bottom-heavy shape.

The amount of ionizing radiation a galaxy produces per unit time is primarily determined by the rate at which it forms stars and the properties of its stellar population (e.g., age, IMF, binarity, and metallicity). For example, the ionizing photon yield, for the same amount of stars, is higher at lower metallicities owing to the higher surface temperatures of such stars in the absence of metal-line cooling. Additionally, it is important to remember that feedback mechanisms arising from preceding stellar populations (whether Pop III or Pop II) would also impact the formation and evolution of the subsequent generation of stars, thereby affecting the emissivity of ionizing photons from a galaxy. Broadly speaking, these feedback processes are classified under the following three headings:

- **Chemical feedback:** This refers to the change in the metallicity of the star-forming gas. The earliest metal-free stars synthesized heavy elements in their cores, which were eventually ejected into the surrounding medium through supernova explosions or stellar winds. The injection of metals alters the chemical composition of the gas, influencing the nature of new stars that are formed and consequently, the amount of ionizing photons they produce.
- **Mechanical feedback:** This refers to the injection of mechanical energy into the interstellar medium by massive stars in the form of stellar winds or supernova explosions. These energetic events can expel loosely bound gas from the potential well of haloes, either partially or completely, thereby suppressing star formation (and thus, the production of ionizing photons) — especially in low-mass systems.
- **Radiative feedback:** This refers to the effects caused by the heating of gas as a result of photoionization. Firstly, if the thermal velocity of the photoionized gas exceeds the escape velocity of the halo, the gas unbinds and can easily stream out from the potential well (a process known as photoevaporation), thereby depleting the gas reservoir in sufficiently low mass systems. Secondly, photoionization heating can also sufficiently raise the gas temperature to a point where its thermal pressure exceeds the gravitational binding energy, preventing gas from being accreted onto these systems.

Until now, we have only discussed the production of ionizing photons by stars within galaxies. However, not all of these photons produced will escape into the surrounding IGM. A portion of them may well be absorbed within the interstellar medium of the galaxy itself, most likely by dense clouds of neutral hydrogen gas. The escape fraction of ionizing photons, also known as Lyman continuum (LyC) photons, depends very sensitively on the density and clumping structure of neutral hydrogen and dust in the interstellar medium (ISM) and circumgalactic medium (CGM) of a galaxy. In the literature, two primary mechanisms of LyC leakage have been proposed - namely, an ionization-bounded nebulae with “holes”, and density-bounded nebulae (Zackrisson et al., 2013). In the first scenario, it is believed that supernovae blast waves or stellar winds carve out low-density tunnels in the neutral ISM, allowing LyC photons to escape without being absorbed. This leads to an anisotropic leakage of ionizing radiation from the star-forming regions. In the second scenario, it is hypothesized that the LyC radiation from an intense starburst event depletes all of the surrounding neutral hydrogen before a full Strömrgren sphere is developed, thereby allowing the ionizing radiation to escape more isotropically.

4.2 Accreting black holes: Quasars

Besides the stellar sources, a population of accreting black holes (namely, quasars) can also produce significant ionizing radiation and may have thus contributed to reionization. Observational studies indicate that the quasar luminosity function peaks at around $z \approx 3$, and exponentially declines at higher redshifts, raising considerable doubt about their contribution to reionization at higher redshifts ($z \geq 6$) (Kulkarni et al., 2019b). Nevertheless, it turns out that several aspects of the reionization process change dramatically if quasars, rather than stars within galaxies, are the primary sources of ionizing radiation.

Firstly, quasars have a much harder ionizing spectrum, producing a significantly higher number of high-energy photons compared to the softer UV radiation from stars. These highly energetic photons, often in the form of hard X-rays (≥ 10 keV), have comparatively longer mean free paths and can thus travel much larger distances through the IGM. Therefore, they would ionize and heat the IGM much more uniformly than stellar radiation. Moreover, these X-ray photons are capable of ionizing more than a single hydrogen atom: the first atom being ionized through regular photoionization, and several other atoms in its vicinity through repeated secondary collisional ionizations caused by the energetic photoelectrons generated from the primary photoionization. While secondary ionizations might seem to boost the

ionization efficiency of quasars, this effect becomes less effective over time. As the ionized fraction in the IGM rises to a few percent, the number of secondary ionizations drops significantly and then, most of the energy from the primary photoelectrons goes into heating the medium through elastic Coulomb collisions. Therefore, lower-energy photons, from either quasars or stars, are still needed to achieve complete ionization of the Universe.

The hard non-thermal spectra, which are characteristic of quasars, further suggest that they are capable of causing the double-reionization of helium (which requires photons with energies > 54.4 eV, not produced in galaxies) almost simultaneously alongside the reionization of hydrogen. Additionally, some of these hard X-ray (≥ 10 keV) photons, with mean free paths comparable to the horizon scale, are rarely absorbed and continue to free-stream redshifting to lower energy bands, and end up contributing to the soft X-ray background (XRB) which we observe at present. As a result, constraints on the unresolved soft (0.5–2 keV) X-ray background place strict limits on the allowed abundance of quasars and their contribution to reionization at $z \geq 6$.

The issue of the contribution of active galactic nuclei (AGN) to reionization witnessed a renewed interest after claims of high number densities of faint AGN at $z \sim 4$ by Giallongo et al. (2019) and Boutsia et al. (2018). When extrapolated to $z \approx 5.6$, these findings suggest that AGN could have played a significant role in reionizing the Universe. Moreover, observational studies at low redshift ($z \approx 3$ –4) show that the escape fraction of ionizing photons from quasars can be significantly higher compared to that from galaxies (Grazian et al., 2018; Romano et al., 2019; Smith et al., 2020). This picture of quasar-driven reionization has recently gained further observational support with the discovery of a population of moderate-luminosity AGN candidates, powered by early supermassive black holes, in deep JWST surveys at redshifts $4 \leq z \leq 13$ (Harikane et al., 2023b; Maiolino et al., 2023; Matthee et al., 2024). Interestingly, the number densities of these JWST-detected AGN are comparatively higher (~ 10 times) than that expected from an extrapolation of the pre-JWST quasar luminosity function to these faint luminosities. In light of these latest observations, a recent analysis by Madau et al. (2024) suggests that AGN at $z > 5$ could reionize the Universe without overproducing the unresolved X-ray background or contradicting HeII Lyman-alpha forest observations, provided their ionizing UV spectrum is exceptionally steep and/or their HeII-ionizing photons (energies > 54.4 eV) are internally absorbed.

4.3 Exotic sources or mechanisms

Besides the conventional astrophysical sources mentioned in the previous sub-sections, various other alternative mechanisms have also been proposed in the literature that could have contributed to the reionization of the IGM. One of the most widely discussed possibilities is the annihilation or decay of dark matter particles (Mapelli et al., 2006; Belikov and Hooper, 2009; Liu et al., 2016). These dark matter interaction processes give rise to standard model particles, such as leptons and baryons, along with the emission of photons (whose exact energy depends on the particle masses involved) that can easily ionize the surrounding neutral atoms. Unlike conventional sources such as galaxies and quasars, ionizing photon production through such processes is not tied to the site of collapsed structures and can take place throughout the Universe, resulting in a more uniform reionization topology. Primordial black holes of intermediate mass (termed as “mini quasars”) at $z > 10$ accreting gas through the Bondi-Hoyle process (Madau et al., 2004; Ricotti and Ostriker, 2004), or stellar-mass black holes in binary systems (“micro quasars”) accreting from their high-mass companion stars (Mirabel et al., 2011), have also been proposed as potential sources of ionizing photons. These early black holes may have contributed to the process of reionization before more conventional sources took over. There have also been studies that argue that a large fraction of stars in high-redshift galaxies probably formed in globular clusters (Ricotti, 2002; Ma et al., 2021), which leak their emitted radiation entirely into the IGM, thereby contributing a substantial fraction of photons for reionization.

5 Observational probes of Reionization

5.1 Cosmic Microwave Background observations

After the first atoms formed, primordial radiation decoupled from matter and traveled mostly unimpeded through the Universe. Today, we observe these photons, originating from the epoch of the last scattering, as the cosmic microwave background (CMB). However, once the first luminous sources began ionizing the IGM, these CMB photons were re-scattered on their way through the IGM by the free electrons produced during reionization, see Figure 4 for an illustration. This scattering reduces the amplitude of the primary temperature anisotropies on angular scales smaller than the horizon scale at the re-scattering epoch by a factor of $e^{-\tau_{\text{el}}}$, where

$$\tau_{\text{el}} = c \sigma_T \bar{n}_H \int_{t_0}^{t_{\text{CMB}}} dt \chi_{\text{He}}(t) Q_{\text{He}}(t) a^{-3}(t) \quad (3)$$

is the integrated electron scattering optical depth of CMB photons. In the above equation, σ_T is the Thomson scattering cross-section, and the integral runs from the present epoch t_0 to the origin of the CMB t_{CMB} . The combination $\bar{n}_H \chi_{\text{He}} Q_{\text{He}} a^{-3}$ represents the density of free electrons, and ensures that its contribution to the integral is essentially zero at epochs before the onset of reionization. As a result of this scattering, the angular power spectrum of CMB temperature anisotropies is damped by a factor of $e^{-2\tau_{\text{el}}}$ on these small angular scales (i.e., high- ℓ), while remaining largely unaffected on larger scales. Unfortunately, this damping is completely degenerate with the amplitude (A_s) of the primordial power spectrum of scalar perturbations and is extremely difficult to discern directly from observations.

Thankfully, the Thompson scattering process also causes the scattered radiation to become linearly polarized when free electrons interact with the incident quadrupolar CMB radiation field. This secondary curl-free (E-mode) polarization is most pronounced on angular scales corresponding to the horizon size at the epoch when the photons were scattered. Therefore, the detection of polarization on scales larger than the angle subtended by the causal horizon at the surface of last scattering (i.e., during cosmological recombination) provides strong evidence

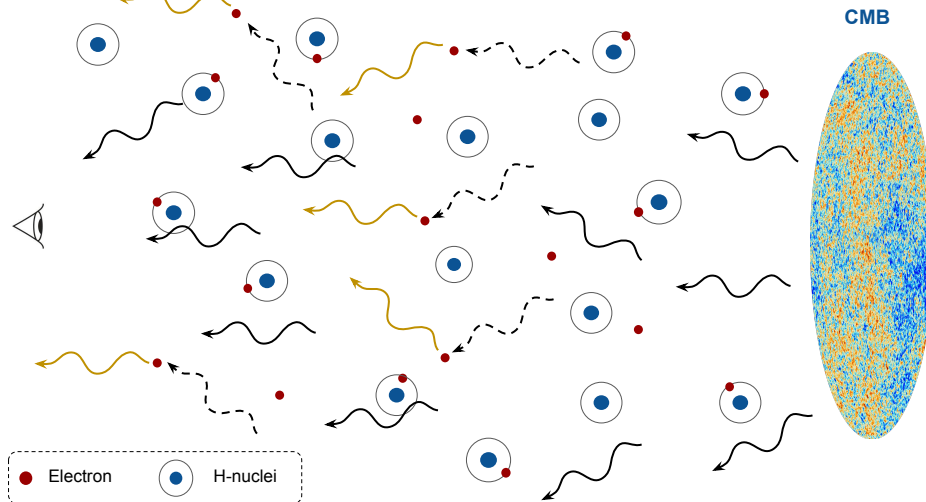


Fig. 4: A cartoon illustration showing the Thomson scattering of CMB photons by free electrons produced during reionization. While the majority of the photons (shown using black solid curves) from the epoch of recombination travel through the IGM unobstructed, some of the photons (shown using black dashed curves) are intercepted by free electrons on their way and get scattered away in random directions (shown using yellow curves).

for Thomson scattering by free electrons in the post-recombination Universe. This feature in the polarization power spectrum at low angular multipoles (low- ℓ) serves as a tell-a-tell sign of cosmic reionization and is generally called the 'reionization bump'. Additionally, similar to the temperature anisotropies, the polarization anisotropies are also suppressed by a factor of $e^{-\tau_{\text{el}}}$ at angular scales larger than the horizon size at the epoch of reionization. Moreover, the location of the reionization bump and its amplitude in the polarization power spectrum depends on when the Universe was reionized and the square of the electron scattering optical depth (τ_{el}). Hence, the shape of the large-scale CMB polarization power spectrum helps in breaking the degeneracy between A_s and τ_{el} , which is expected to exist in measurements of temperature anisotropies as described above. Calculating the value of τ_{el} from observations of the CMB temperature (T) and polarization (E) auto-correlation and cross-correlation power spectra requires adopting a model for the redshift evolution of the number density of free electrons, or equivalently, a model for reionization. For instance, the latest measurement of the electron scattering optical depth at $\tau_{\text{el}} = 0.054 \pm 0.007$ reported by Planck Collaboration et al. (2020) has been obtained from a combined analysis of the full Planck mission TT ($2 \leq \ell \leq 2500$), TE ($30 \leq \ell \leq 2000$) and EE ($2 \leq \ell \leq 2000$) data and the Planck CMB lensing data ($8 \leq \ell \leq 400$), assuming a tanh model for reionization, which is parametrized by a reionization midpoint z_{re} and a redshift width Δz_{re} (kept fixed to a value of $\Delta z_{\text{re}} = 0.5$)¹. In this case, the measured value of τ_{el} corresponds to a reionization "midpoint" of $z_{\text{re}} = 7.7 \pm 0.7$. However, it is important to realize that this simplified redshift-symmetric tanh model of reionization, widely adopted in the standard analysis of CMB data, greatly differs in shape from both physical and empirical models of reionization history, which are based on hierarchical models of structure formation and/or inferred from other high-redshift astrophysical observables (Paoletti et al., 2024). Moreover, the value of the optical depth, in principle, could also depend on the details of the reionization history assumed (e.g., see Hazra and Smoot (2017); Miranda et al. (2017); Qin et al. (2020); Planck Collaboration et al. (2020); Chatterjee et al. (2021)).

Reionization also produces additional temperature anisotropies in the CMB spectrum on small scales which offer complementary information about the process compared to large-angle polarization measurements that are largely insensitive to its patchiness and duration. The bulk motion of free electrons in ionized bubbles relative to the CMB rest frame causes a Doppler shift in the scattered photons, leading to a small shift in the observed CMB temperature. This phenomenon is known as the kinetic Sunyaev-Zel'dovich (kSZ) effect. In the non-relativistic limit, the temperature change is proportional to the line-of-sight bulk velocity of the electrons and the number density of free electrons. We emphasize that the kSZ effect (which arises from the bulk motion of free electrons) is fundamentally different from the thermal Sunyaev-Zel'dovich (tSZ) effect, which arises due to the Compton scattering of CMB photons inside hot gas residing in large-scale structures such as galaxy clusters.

The kSZ signal broadly encompasses two distinct components, the homogeneous kSZ and the patchy kSZ. The homogeneous kSZ signal arises from spatial inhomogeneities in the baryonic density in the fully ionized universe. In contrast, the patchy kSZ signal is driven by fluctuations in the ionization fraction during the EoR. The amplitude of the patchy kSZ power spectrum is primarily determined by the timing and duration of reionization, while its shape depends on the size distribution of the ionized bubbles. Several studies in the literature have discussed the prospects of using the patchy kSZ signal for inferring not only the mid-point and duration of reionization but also the

¹In the tanh parameterization of reionization, the evolution of the globally averaged free electron fraction x_e as function of redshift (z) is given by the following mathematical expression - $x_e(z) = \chi_{\text{He}}(z) Q_{\text{HII}}(z) = \frac{1}{2} \left[1 + \tanh \left(\frac{y(z_{\text{re}}) - y}{\Delta y} \right) \right]$, where $y(z) = (1+z)^{3/2}$, $\Delta y = 1.5 \sqrt{1+z_{\text{re}}} \Delta z_{\text{re}}$ and other symbols have their usual meaning

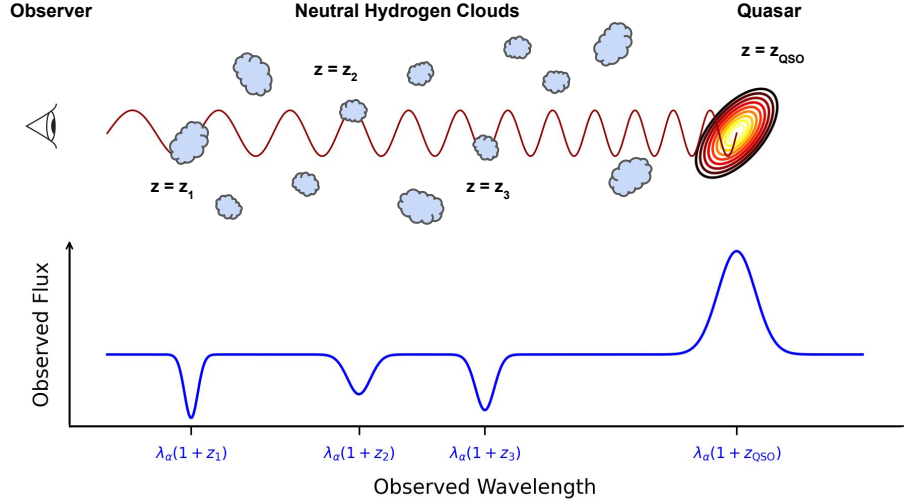


Fig. 5: A cartoon illustration of the Lyman- α forest observed in the spectra of distant sources. This arises due to the absorption of the radiation emitted by a background source as it passes through multiple clouds of neutral hydrogen along the line of sight.

sources driving the process (Park et al., 2013; Gorce et al., 2020; Paul et al., 2021; Nikolić et al., 2023; Jain et al., 2024). Recently, the first 3σ detection of the kSZ signal was reported by Reichardt et al. (2021) using the temperature and polarization data (measured across the multipole range - $2000 \leq \ell \leq 11,000$) from the SPT-SZ and SPT-pol surveys, yielding a value of $D_\ell^{\text{kSZ}} = \ell(\ell + 1)C_\ell^{\text{kSZ}} = 3 \pm 1 \mu\text{K}^2$ at an angular multipole of $\ell = 3000$.

5.2 Lyman-alpha absorption studies

Absorption lines seen in the spectra of distant astronomical sources provide an elegant way to study the physical state of the intervening medium at different redshifts along a particular line of sight. Among the various sources known to exist in the early Universe, quasars are believed to emit strongly across a wide range of wavelengths, with their intrinsic spectrum showing broad emission lines superimposed on a smooth continuum. As these emitted photons travel towards us, their wavelengths are stretched due to the expansion of the Universe. Eventually, photons that were emitted with rest-frame wavelengths shorter than the Lyman- α wavelength ($\lambda_\alpha = 1216 \text{ \AA}$) will get redshifted close to the Lyman- α transition wavelength at some point on their way. If this occurs at a region in the IGM where there are substantial neutral hydrogen atoms, the atoms will absorb these photons, transitioning from the ground state to the first excited state (i.e., undergoing the $1s \rightarrow 2p$ Lyman- α transition) and then again de-excite, re-emitting the photons in random directions. This resonant scattering results in an absorption line in the observed quasar spectra blueward of the rest-frame Lyman- α emission. For an absorption system at some intermediate redshift z_{abs} (where, $0 < z_{\text{abs}} < z_{\text{source}}$) along the line of sight, we would expect absorption signatures in the observed spectrum at a wavelength of $(1 + z_{\text{abs}})\lambda_\alpha$. The presence of multiple intergalactic clouds of neutral hydrogen lying at different redshifts along the path would then leave a series of narrowly spaced absorption lines in the observed spectrum, which are collectively referred to as the Lyman- α forest (see Figure 5 for an illustration). On the other hand, photons emitted with rest-frame wavelengths $\lambda > \lambda_\alpha$ will have their wavelengths redshifted further and further away from the Lyman- α resonance as they travel toward us, and therefore will never be absorbed by any intervening neutral hydrogen. As a result, a sharp decrease in flux is expected across the position of Lyman- α emission line in the observed spectrum if there is neutral hydrogen present between the quasar and us. This is known as the *Gunn-Peterson (GP) effect* (Gunn and Peterson, 1965). It should be emphasized that imprints of Lyman- α absorption features due to a neutral IGM on observed spectra are not limited to quasars; this effect applies equally to any distant background source, such as primeval galaxies and gamma-ray burst afterglows.

The key observable in quasar absorption spectra is the transmitted flux $F_\alpha = e^{-\tau_\alpha}$, where

$$\begin{aligned} \tau_\alpha(\lambda_{\text{obs}}, z) &= \frac{\sigma_\alpha c}{H(z)} x_{\text{HI}} n_H (1+z)^3 \\ &\approx 2.3 \times 10^5 x_{\text{HI}} \left(\frac{n_H}{\bar{n}_H} \right) \left(\frac{\Omega_b h^2}{0.022} \right) \left(\frac{\Omega_m h^2}{0.142} \right)^{-1/2} \left(\frac{1-Y}{0.76} \right) \left(\frac{1+z}{5} \right)^{3/2} \end{aligned} \quad (4)$$

is the optical depth, due to Lyman- α absorption at the absorption redshift z ($\equiv \lambda_{\text{obs}}/\lambda_\alpha - 1$), observed today at a wavelength of λ_{obs} . In the above expression, σ_α is the Lyman- α absorption cross-section, x_{HI} is the neutral hydrogen fraction, and $H(z)$ is the Hubble parameter. In deriving these expressions, we have neglected the width of the absorption cross-section and effects due to peculiar velocities for simplicity. We have also approximated $H(z) \approx H_0 \Omega_m^{1/2} (1+z)^{3/2}$ in the second expression, valid for $z \gtrsim 2$. When the IGM is highly ionized, the residual neutral fraction x_{HI} can be related to the thermal state of the IGM and the background photoionization rate Γ_{HI} assuming an equilibrium

between photoionization and recombination, valid for low-density gas that forms the Lyman- α forest -

$$x_{\text{HI}} = \frac{\alpha_R(T) \chi_{\text{He}} n_H (1+z)^3}{\Gamma_{\text{HI}}}. \quad (5)$$

While the global neutral hydrogen fraction \bar{x}_{HI} can be directly inferred from the average optical depth $\bar{\tau}_\alpha$, we remind the readers that the main observable is the average transmitted flux $\bar{F}_\alpha \neq e^{-\bar{\tau}_\alpha}$, complicating direct inferences of \bar{x}_{HI} from quasar observations. Nonetheless, it is clear from equation (4) that Lyman- α absorption is highly sensitive to the neutral hydrogen density. For instance, a neutral hydrogen fraction of $x_{\text{HI}} \approx 10^{-4}$ results in $\tau_\alpha \gg 1$, causing the transmitted flux to approach zero ($F_\alpha \rightarrow 0$). This results in extended absorption “troughs” blueward of the Lyman- α emission in the observed spectrum. The absence of a GP trough only provides an upper limit on x_{HI} . Observations showing no such troughs at $z \lesssim 5$ suggest the IGM is highly ionized at these redshifts. Thus, the Lyman- α forest is a powerful probe of the late stages of reionization, when the IGM is predominantly ionized with only minor amounts of residual neutral hydrogen. However, for higher neutral fractions $x_{\text{HI}} \gg 10^{-3}$, the quasar absorption spectra show minimal transmitted flux, making interpretation of the observations at higher redshifts challenging without detailed theoretical models.

Recent spectroscopic observations of high-redshift quasars at $5 \lesssim z \lesssim 6$ have revealed significant variation in the average transmitted flux across different sight lines (Becker et al., 2015; Bosman et al., 2018, 2022). These fluctuations are larger than those expected in standard models with uniform ionizing backgrounds and power-law temperature-density relations. As a result, a number of models that invoked fluctuations in the temperature (D’Aloisio et al., 2015), background photoionization rate (Davies and Furlanetto, 2016) and density distribution (Chardin et al., 2017) were proposed. However, a delayed end to reionization at $z \approx 5$ seemed to most satisfactorily explain the observed scatter in the transmitted flux, as such a scenario would leave large “islands” of neutral hydrogen even at $z < 6$ that could cause significant absorption along certain quasar sight lines (Kulkarni et al., 2019a; Nasir and D’Aloisio, 2020).

A complementary method of constraining the neutral fraction towards the end of reionization is by analyzing the “dark pixels”, which entails measuring the fraction of pixels that are entirely absorbed in the observed Lyman- α forest spectra. This offers a relatively model-independent estimate of the filling factor of ionized regions (McGreer et al., 2015; Jin et al., 2023). However, this method gives only an upper limit on \bar{x}_{HI} , as residual HI inside ionized regions (in place of neutral regions in the IGM) may also saturate the Lyman- α forest.

Since the reionization process is patchy, small highly-ionized regions are expected to exist even when the Universe is still largely neutral. These regions would manifest as sharp “spikes” of transmission in the spectra of high-redshift quasars. The position and spacing of these spikes, interspersed with regions of no detectable flux (known as “dark gaps”), are expected to hold more information than what can be captured by just measuring the effective optical depth. Studies have shown that the number and height of these transmission spikes are sensitive to the ionization fraction of the IGM, which in turn depends on the photoionization rate and the temperature of the gas in the ionized regions (Gaikwad et al., 2020). On the other hand, the size distribution of these so-called dark gaps has also been claimed to be a robust diagnostic of the ionization state of the IGM during late stages of reionization (Gallerani et al., 2006, 2008; Zhu et al., 2021). However, these methods of estimating \bar{x}_{HI} are usually model-dependent, requiring several assumptions to be made.

Quasars not only act as backlights for absorption studies but also create extensive ionized regions around themselves, where the strength of the ionizing radiation field is higher than average. These regions, known as proximity zones, are the only areas where significant transmission occurs just blueward of the quasar’s Lyman- α emission. If the sizes of these proximity zones can be reliably measured from absorption spectra, they could provide information about the amount of neutral hydrogen in the IGM around the quasar (Fan et al., 2006; Bolton and Haehnelt, 2007; Carilli et al., 2010). However, inferences of x_{HI} drawn from observed quasar proximity zones depend on associated assumptions regarding the intrinsic properties of quasars, such as their ionizing luminosity and age.

Observations of the mean Lyman- α transmitted flux, combined with numerical simulations, have also helped estimate the HI photoionization rate Γ_{HI} . In such studies, one essentially tries to match the mean transmission in the simulated spectra to the observational measurements at $5 < z < 6$, since we expect $\tau_\alpha \propto \Gamma_{\text{HI}}^{-1}$ to hold in photoionization equilibrium (see equations (4) and (5)). However, the photoionization rate estimated through such a procedure depends on the assumptions made regarding the mean free path λ_{mfp} of ionizing photons and the temperature-density relation in the low-density IGM. In recent times, it has also been possible to measure λ_{mfp} directly from quasar absorption spectra, which suggests that reionization is likely to complete only by $z \sim 5.3$ (Zhu et al., 2023). Such measurements of λ_{mfp} and Γ_{HI} can be used to obtain an estimate of the number of ionizing photons available in the IGM (since, $\dot{n}_{\text{ion}} \propto \Gamma_{\text{HI}}^{-1} \lambda_{\text{mfp}}$) (e.g., Gaikwad et al., 2023).

Reionization can also be constrained through the thermal history of the IGM, measured using quasar absorption spectra. The power spectrum of Lyman- α absorption fluctuations shows small-scale suppression due to pressure smoothing, which depends on the thermal evolution of the gas (Rorai et al., 2017; Walther et al., 2019). Recent studies (e.g., Gaikwad et al., 2020) have measured the IGM temperature using transmission spikes at $z \sim 5.5$, allowing constraints on the reionization history through comparisons with a theoretical model (Maity and Choudhury, 2022).

5.3 High-redshift galaxies: Lyman-break galaxies and Lyman-alpha emitters

As mentioned previously, the high volume densities of star-forming galaxies at high redshifts make them the most favored source of ionizing photons. Therefore, to reliably trace the course of reionization, it is essential to first obtain a census of the Lyman continuum photons contributed by them for ionizing hydrogen in the IGM. However, directly measuring the ionizing radiation produced from such early galaxies escaping into the IGM is extremely challenging if not impossible. This difficulty arises due to the presence of substantial amounts of neutral hydrogen gas in their ISM and the IGM, both of which absorb the produced LyC radiation.

Because of these difficulties, the total ionizing radiation contributed by galaxies for reionization is usually estimated indirectly by

combining three different pieces of information, namely, the rest-frame UV luminosity density, an efficiency factor ξ_{ion} that translates the non-ionizing UV luminosity of galaxies to their Lyman-continuum radiation, and the escape fraction f_{esc} .² Without any loss of generality, we can write the ionizing emissivity of galaxies which appears as the source term in equation (1) to be,

$$\begin{aligned} \dot{n}_{\text{ion}} &\equiv \frac{dn_{\text{ion}}}{dt} = \int dL_{\text{UV}} \Phi(L_{\text{UV}}) \dot{N}_{\text{ion}}(L_{\text{UV}}) f_{\text{esc}}(L_{\text{UV}}), \\ &= \int dL_{\text{UV}} \Phi(L_{\text{UV}}) L_{\text{UV}} \xi_{\text{ion}}(L_{\text{UV}}) f_{\text{esc}}(L_{\text{UV}}), \end{aligned} \quad (6)$$

where $\dot{N}_{\text{ion}} \equiv L_{\text{UV}} \xi_{\text{ion}}$ represents the number of ionizing photons produced per unit time by a galaxy with UV luminosity L_{UV} and $\Phi(L_{\text{UV}})$ denotes the UV luminosity function of galaxies, which quantifies the abundances of galaxies in a given comoving volume per unit luminosity interval. It must be noted that the integral above formally extends down to the faintest of galaxies that are capable of producing ionizing photons. These ultra-faint galaxies are unlikely to be individually detectable in current or future galaxy surveys and therefore the observed UV luminosity function would need to be extrapolated down to lower luminosities, introducing uncertainties to the contribution of faint galaxies towards reionization.

Over the past decade, the commissioning of large galaxy surveys using space-based and ground-based telescopes like the James Webb Space Telescope (JWST), the Hubble Space Telescope (HST), the Spitzer Space Telescope, the Subaru Telescope (Bouwens et al., 2015, 2017; Atek et al., 2018; Ono et al., 2018; Bowler et al., 2020; Harikane et al., 2022; Donnan et al., 2023; Harikane et al., 2023a; Bouwens et al., 2023; McLeod et al., 2024; Donnan et al., 2024; Whittler et al., 2025) has resulted in a growing sample of high redshift galaxies. A widely used method for detecting high-redshift galaxies leverages the distinctive spectral break caused by the absorption of emitted photons by intergalactic and interstellar neutral hydrogen along the line of sight. Therefore, the light emitted blueward of a Lyman-series transition has an extremely low probability of reaching us, making the galaxy distinct in different broadband filters of the telescope. Galaxies selected using this technique are called the Lyman-break galaxies (LBGs). These galaxy observations have been instrumental in obtaining robust measurements of the rest-frame UV luminosity function $\Phi(L_{\text{UV}})$ of galaxies at high redshifts ($6 < z < 10$) and more recently, even out to redshifts as high as $z \approx 15$.

The second most crucial ingredient for calculating the ionizing photon budget from galaxies is the production efficiency of ionizing radiation (ξ_{ion}), which depends on the spectral energy distribution of the stellar population in high- z galaxies. Several theoretical stellar population synthesis (SPS) studies (Liu et al., 2024; Wilkins et al., 2016) have shown that the number of ionizing photons produced depends strongly on the choice of the SPS model (isolated or binaries) and astrophysical factors such as stellar age, stellar metallicity, stellar IMF, mode of star-formation etc. On the observational front, with the growing number of line-emitting galaxies and advancements in spectroscopy, it has been possible to obtain a lower bound on ξ_{ion} based on the measured intensity of nebular emission lines (such as Balmer lines) in galaxy spectra along with certain assumptions about the recombination process. Using JWST observations of high- z galaxies, several studies initially inferred values of $\log_{10} [\xi_{\text{ion}}/(\text{ergs}^{-1} \text{ Hz})]$ in the range of 25.5 – 26.0 (Curtis-Lake et al., 2023; Rinaldi et al., 2023; Endsley et al., 2023; Atek et al., 2024; Simmonds et al., 2024a; Álvarez-Márquez et al., 2024; Calabro et al., 2024), which were considerably higher than the canonical values $\log_{10} [\xi_{\text{ion}}/(\text{ergs}^{-1} \text{ Hz})] \approx 25.2$ obtained from previous studies with the HST (Robertson et al., 2015) (though, also see Matthee et al. (2023); Simmonds et al. (2024b); Begley et al. (2025)). Some of these studies have also reported an increasing trend of ξ_{ion} towards higher redshifts and fainter galaxies.

The last but perhaps the most important ingredient for reionization history calculations is the escape fraction, which is completely degenerate with ξ_{ion} . A direct observational estimate of f_{esc} during reionization is impossible for the reasons outlined earlier in this section. Consequently, indirect estimators of f_{esc} are used - mostly, derived from detailed studies of correlations between LyC leakage and various galaxy properties in low-redshift analogs of LyC leakers (Flury et al., 2022; Choustikov et al., 2024). Some of the different diagnostics proposed include high [OIII]/[OII] (O_{32}) ratios (Jaskot and Oey, 2013; Nakajima and Ouchi, 2014; Izotov et al., 2018), UV continuum slope (Chisholm et al., 2022), velocity separation between Lyman- α peaks (Verhamme et al., 2015, 2017; Izotov et al., 2018, 2021), Lyman- α equivalent width (Steidel et al., 2018; Pahl et al., 2021; Begley et al., 2022) and so on. However, it must be remembered that many of these indirect estimators could suffer from degeneracies related to stellar properties like age, metallicity, etc.

Combining these, it becomes straightforward to obtain the total ionizing emissivity of galaxies at a given redshift and also study the relative contribution of galaxies towards this photon budget as function of luminosity. These observations therefore hold the promise of resolving the long-standing debate about the contribution of low-luminosity galaxies to the ionizing photon budget for reionization. In the literature, some studies (Sharma et al., 2016; Naidu et al., 2020; Joshi and Sharma, 2024) contend that faint galaxies (having magnitude $M_{\text{UV}} \geq -17$) make only a negligible contribution, while others (Anderson et al., 2017; Lewis et al., 2020; Atek et al., 2024; Chakraborty and Choudhury, 2024; Simmonds et al., 2024a) argue that these sources play a dominant role in the reionization of the Universe.

Given the intricate interplay between cosmic reionization and galaxy formation, it is natural to expect that cosmic reionization would also leave noticeable imprints on both the physical and statistical properties of galaxies. In addition to shedding light on the contribution of different galaxies to the reionization photon budget via equation (6), these galaxy surveys offer crucial insights into star formation activity and the properties of stellar populations in early galaxies. For instance, the rest-frame UV continuum emission (1250–1500 Å), which gets redshifted into optical wavelengths by the time it reaches us, serves as a measure of its instantaneous star formation rate, since UV

²Strictly speaking, this escape fraction f_{esc} refers to the relative fraction of ionizing photons escaping from galaxies to the fraction of 1500 Å UV-continuum photons that escaped.

radiation is primarily emitted by massive, hot stars that are short-lived. Another higher-order summary statistic that has recently become available at high redshifts from such surveys is the two-point correlation function which quantifies the clustering of a galaxy population in two- or three-dimensional space. The topology and morphology of reionization depend crucially on how the ionizing sources are distributed in space. Star formation and ionizing photon production are also influenced by feedback mechanisms, including radiative feedback from cosmic reionization. This feedback, which heats gas and suppresses star formation in low-mass haloes, is expected to flatten or turn over the faint end of the galaxy UV luminosity function. Any detection of such a feature in the luminosity function will help better understand the feedback mechanisms.

A complementary approach which is now increasingly used for detecting star-forming galaxies at high redshifts is based on the identification of redshifted line emission within a narrow redshift range from narrow-band imaging or spectroscopic observations. Galaxies that are selected using this technique are called line-emitting galaxies. Among the various line emissions expected from high-redshift galaxies, the Lyman- α line, which results from the recombination of ionized hydrogen in star-forming regions, is perhaps the most promising for such searches owing to its high intrinsic strength. Galaxies selected using their strong Lyman- α emission are known as Lyman-alpha emitters (LAEs).

The sensitive dependence of Lyman- α transmission on the presence of neutral hydrogen (HI) around galaxies or in the IGM makes LAEs a promising probe of cosmic reionization (Dijkstra, 2014; Ouchi et al., 2020). Galaxies are believed to form in overdense regions of the Universe, which are also the first to be reionized. Consequently, Lyman- α photons emitted by galaxies within HII regions can traverse through the ionized bubble, redshifting away from line resonance, before encountering the neutral IGM. Due to the strong frequency dependence of the Lyman- α absorption cross-section, these emergent photons are then less likely to be scattered out of the line of sight, allowing a substantial fraction of them to reach the observer. Therefore, crudely speaking, the visibility of galaxies in Lyman- α can be used to draw inferences about the presence of neutral hydrogen in the intervening medium.

With the progress of reionization, larger HII regions form around galaxies, increasing the prospects of detecting a higher number of galaxies emitting in Lyman- α . As a result, the Lyman- α luminosity function of LAEs is expected to show a sharp drop in amplitude with increasing redshift (where the IGM becomes increasingly neutral). This distinctive evolution in the abundance of LAEs, as opposed to the LBGs over similar redshifts, can help in constraining the timing of reionization, assuming that the intrinsic Lyman- α properties of galaxies do not significantly change. Given the fact that the Lyman- α emission from galaxies within large ionized bubbles remains (relatively) unattenuated compared to that from galaxies located elsewhere (such as inside small ionized bubbles or neutral regions), it is only to be expected that the narrow-band Lyman- α searches will preferentially detect galaxies residing in the ionized regions of the IGM. Therefore, the “observed” spatial distribution of LAEs is expected to be modulated by the large-scale ionization field. With the ionized regions becoming increasingly rare at higher redshifts, one anticipates that the clustering of LAEs (quantified by the amplitude of its two-point correlation function) should also increase with increasing redshift. Unfortunately, the interpretation of observations of LAEs at high redshifts is not straightforward and plagued by several uncertainties such as the amount of relative velocity shift of the Lyman- α emission line as it emerges from the source, the density distribution and the size of ionized regions around these sources, etc., thereby requiring detailed theoretical models.

In the last decade, sensitive narrowband surveys with the Subaru Telescope have been successful in increasing the sample of high-redshift LAEs, enabling robust determination of the Lyman- α LFs and LAE clustering, which agree well with the theoretical expectations outlined above (Konno et al., 2018; Itoh et al., 2018; Goto et al., 2021). More recently, observations with the JWST have pushed the boundaries of high- z LAE studies even further by facilitating the detection of numerous LAEs and allowing for their detailed characterization deep into the EoR (Witstok et al., 2024b; Tang et al., 2024; Jones et al., 2024). The most exciting result of the lot has been the detection of Lyman- α emission from galaxies at redshifts as high as $z = 10.6$ (GNz-11; Bunker et al., 2023) and $z = 13$ (JADES-GS-z13-1-LA; Witstok et al., 2024a), when the Universe is significantly neutral. Some of the latest studies (e.g., Endsley and Stark, 2022; Whittle et al., 2024) have suggested the presence of large galaxy overdensities around some of the stronger Lyman- α emitters at $z > 6$, lending support to the notion that such overdensities would be easily able to source sufficiently large-sized ionized bubbles, which in turn would facilitate Lyman- α transmission.

5.4 21 cm Emission

The Lyman- α transition presents a significant hurdle in probing the early and intermediate stages of reionization since even a tiny amount of neutral hydrogen (around 1 part in 100,000) can make the IGM entirely opaque to Lyman- α radiation. Similarly, CMB probes are integrated measurements of the ionization state along the line of sight, offering no insights into the intricate details of the reionization process. In this context, an attractive alternative to probe the different stages of reionization is the so-called 21 cm radiation arising from the hyperfine transition in the ground state of neutral hydrogen atoms. More specifically, when the spins of the proton and electron in a neutral hydrogen atom switch between parallel (triplet state) and anti-parallel (singlet state) configurations, the atom emits or absorbs a photon with a rest-frame wavelength of 21.1 cm (i.e., equivalent to a rest-frame frequency of 1420.4 MHz). However, the strength of the 21 cm line transition is extremely weak because the probability of spontaneous emission is low, making them harder to detect unless they are produced from regions with a high number of neutral atoms or those that are exceptionally dense. The optical depth (τ_{21}) of the diffuse IGM towards 21 cm radiation at a redshift z is thankfully extremely low - several orders of magnitude smaller than that of Lyman- α photons.

When background radiation passes through a patch of neutral hydrogen gas at redshift z , 21 cm photons can either be absorbed from or emitted into this radiation. This is entirely dependent on the spin temperature (T_S) of the neutral hydrogen gas, which is defined by the number of hydrogen atoms in the triplet and singlet states. Usually, the primary source of background radiation is the CMB. If the spin temperature is higher than the CMB temperature, the hydrogen will emit 21 cm radiation; conversely, if the spin temperature is lower, the

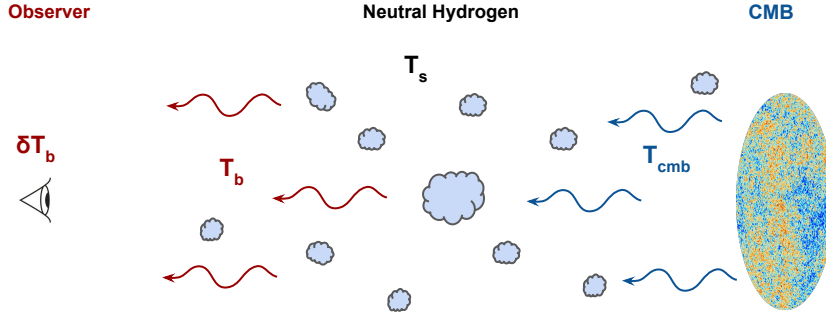


Fig. 6: A cartoon illustration showing the emission or absorption of 21 cm photons by intergalactic patches of neutral hydrogen with a spin temperature of T_S , when irradiated by a background radiation (CMB) having brightness temperature of T_{CMB} .

hydrogen will absorb the 21 cm photons from the CMB. This 21 cm radiation, which gets redshifted into very low radio wavelengths by the time it reaches us, is usually measured relative to the CMB radiation field and expressed in terms of a differential brightness temperature, δT_b (see Figure 6 for an illustration).

The brightness temperature associated with the radiation emerging from neutral regions in the IGM is given by $T_b(z) = T_{\text{CMB}} e^{-\tau_{21}} + T_S(1 - e^{-\tau_{21}})$. Hence, the differential brightness temperature observed at a frequency ν_{obs} along a line of sight \hat{n} relative to the CMB can be expressed as,

$$\begin{aligned} \delta T_b(\nu_{\text{obs}}, \hat{n}) &= \frac{T_b(z) - T_{\text{CMB}}(z)}{1+z} \\ &\simeq 27 \text{ mK } x_{\text{HI}}(\mathbf{x}, z) [1 + \delta(\mathbf{x}, z)] \left(1 - \frac{T_{\text{CMB}}(z)}{T_S(\mathbf{x}, z)} \right) \left(1 + \frac{1}{H(z)} \frac{dv_p}{dr} \right)^{-1} \left(\frac{1+z}{10} \right)^{1/2} \left(\frac{Y_H}{0.76} \right) \left(\frac{0.14}{\Omega_m h^2} \right)^{1/2} \left(\frac{\Omega_b h^2}{0.022} \right), \end{aligned} \quad (7)$$

where we have assumed that the optical depth τ_{21} of 21 cm radiation is much less than unity (the so-called ‘‘optically thin’’ limit). In the above expression, $\mathbf{x} = r_c \hat{n}$ is the comoving distance along the line of sight to redshift z ($\equiv 1420 \text{ MHz}/\nu_{\text{obs}} - 1$) while quantities $x_{\text{HI}}(\mathbf{x}, z)$ and $\delta(\mathbf{x}, z)$ denote the neutral hydrogen fraction and the density contrast of baryonic gas respectively at point \mathbf{x} and redshift z . The quantity dv_p/dr denotes the gradient of the proper velocity projected to the line of sight. The spin temperature of the neutral hydrogen gas in the IGM is represented by the quantity T_S , whereas $T_{\text{CMB}}(z) = 2.73(1+z)$ K denotes the CMB brightness temperature at redshift z .

By the time reionization begins, the IGM has already been significantly heated, primarily by X-ray photons (and to a lesser extent, by UV photons) from the first luminous sources. This causes the spin temperature of neutral hydrogen, which is coupled to the gas kinetic temperature, to be much higher than the CMB temperature and therefore, we observe the differential 21 cm signal in emission during the EoR. During this time, the evolution and fluctuations of the differential brightness temperature are essentially driven by the corresponding evolution and fluctuations in the gas density and ionization structure of the IGM and the peculiar velocities of the gas along the line of sight.

There are two main observational techniques for detecting the cosmological 21 cm signal from the Epoch of Reionization. The first method involves measuring the average intensity of 21 cm radiation across the entire sky as a function of frequency, known as the global 21 cm signal. The second approach focuses on detecting variations in the intensity of 21 cm radiation over a large region of the sky. This method not only aims to statistically detect the signal using summary statistics like the power spectrum or bispectrum but also strives to produce three-dimensional 21 cm images of the IGM during this epoch.

The strength and shape of the global 21 cm signal carry important information about the timing of key cosmic events, such as the formation of the first stars, the onset of cosmic heating by these stars, and the beginning of reionization (Figure 7 shows the evolution of the 21 cm signal in a typical model of cosmic dawn and reionization). However, the 21 cm fluctuations are expected to provide far more detailed insights, particularly regarding the abundance, nature, and distribution of the sources driving reionization, as well as the physical state of the IGM, that cannot be captured using only the globally averaged quantities. For example, the large-scale 21 cm power spectrum is expected to peak on spatial scales corresponding to the characteristic size of ionized regions at that epoch. However, a key difficulty in detecting the 21 cm line is that the cosmological signal is many orders of magnitude smaller than the astrophysical foreground signal arising from galactic and extra-galactic synchrotron and free-free emissions. There has been considerable work to explore ways to remove or avoid these foregrounds and extract the underlying signal. Another possible way to mitigate some part of the foreground contamination is to cross-correlate the 21 cm observations with other high- z observables such as galaxies, which are not expected to exhibit any correlation

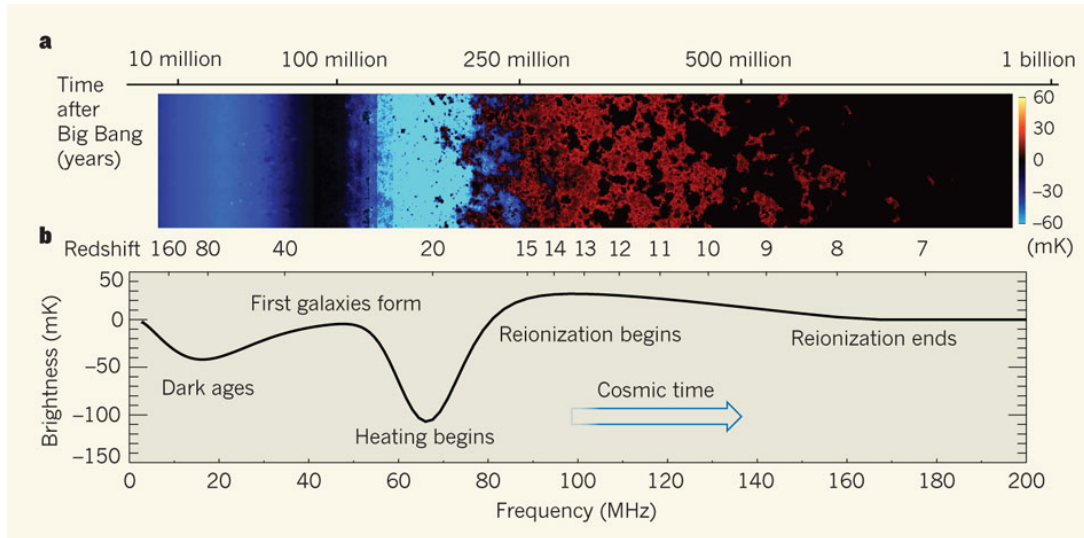


Fig. 7: The evolution of the brightness temperature of the 21 cm radiation, seen relative to the CMB temperature, as a function of time for a typical model of reionization and cosmic dawn. The upper panel shows the evolution of the strength of the spatial fluctuations in the 21 cm brightness temperature along a particular line of sight from a cosmological simulation while the lower panel shows the evolution of the sky-averaged 21 cm global signal, highlighting the key cosmic epochs beginning from the formation of the first stars and galaxies up to the completion of reionization. Image Credits: Pritchard and Loeb (2010)

with the 21 cm foreground signal. Such synergetic approaches are expected to not only provide unambiguous confirmation of any putative detection of the 21 cm signal based solely on statistical auto-correlation studies but also offer independent insights about the drivers and topology of reionization (Lidz et al., 2009; Hutter et al., 2023).

Currently, several interferometric experiments, including the Low Frequency Array (LOFAR) (Gehlot et al., 2019; Mertens et al., 2020), Murchison Widefield Array (MWA) (Barry et al., 2019; Trott et al., 2020), Precision Array for Probing the Epoch of Reionization (PAPER) (Parsons et al., 2010; Abdurashidova et al., 2022), and Hydrogen Epoch of Reionization Array (HERA) (Kolopanis et al., 2019), are focused on detecting the power spectrum of 21 cm fluctuations. These efforts are complemented by global 21 cm experiments, such as the Shaped Antenna measurement of the background Radio Spectrum (SARAS) (Singh et al., 2022), Experiment to Detect the Global EoR Signature (EDGES) (Bowman et al., 2018), and Radio Experiment for the Analysis of Cosmic Hydrogen (REACH) (de Lera Acedo et al., 2022), which aim to measure the 21 cm global signal over a wide range of epochs spanning both the Epoch of Reionization and Cosmic Dawn. In the near future, upcoming telescopes like the Square Kilometer Array (SKA) (Koopmans et al., 2015), with their extremely high resolution and sensitivity, will most likely revolutionize the field of 21 cm cosmology by providing us with a comprehensive 3D tomographic view of the IGM during reionization.

5.5 Fast Radio Bursts

Another promising probe for studying reionization that has gained significant attention in recent years is the use of fast radio bursts (FRBs). FRBs are extremely bright ($\sim 10^{-26}$ watts per square metre per hertz) and short-duration (\sim millisecond) pulses of radio emission coming from extragalactic distances. As these pulses travel towards us, they get dispersed due to their interaction with free electrons in the intervening medium. The amount of dispersion suffered, quantified by the Dispersion Measure (DM), directly depends on the free electron content along its path. For a cosmological FRB, the dominant contribution to its total observed DM is expected to arise from the intergalactic medium (DM_{IGM}), with additional contributions resulting from the host galaxy and the Milky Way. As reionization will only influence the IGM contribution (DM_{IGM}) to the total “observed” DM, it is essential to accurately characterize the other two contributory sources when using FRBs to study the EoR.

Therefore, an ensemble of localized FRBs spread out over the reionization epoch, having precise intergalactic DM measurements and independent redshift estimates from optical observations, can in principle be used to fetch information about the reionization history with

the help of simplistic estimators such as the sky-averaged intergalactic DM (i.e., $\langle \text{DM}_{\text{IGM}} \rangle(z)$) or the redshift derivative of the sky-averaged intergalactic DM (i.e., $d\langle \text{DM}_{\text{IGM}} \rangle/dz$) (Beniamini et al., 2021; Heimersheim et al., 2022; Shaw et al., 2024; Maity, 2024). Interestingly, some studies (e.g., (Fialkov and Loeb, 2016)) have argued that a series of measurements of $\langle \text{DM}_{\text{IGM}} \rangle$ at various cosmic epochs up to some given redshift z can be used to determine the mean integrated Thomson scattering optical depth out to the same redshift, $\tau(z)$ since both these quantities are integrals of the electron number density with slightly different redshift-weight factors. Building on this idea, they propose that integrating this $\tau - \text{DM}$ relation over the entire range of DMs up to the maximum observed DM_{IGM} in a sample of localized FRBs, spanning the period from the onset of reionization to the present day, could provide independent constraints on the total electron scattering optical depth (τ_{el}) of CMB photons (Fialkov and Loeb, 2016).

6 Conclusion

Studying the epoch of reionization is crucial to understanding the early Universe and the formation of the first luminous objects, such as stars, galaxies, and quasars. This period, which began a few hundred million years after the Big Bang, marks a transformative phase in cosmic history when the neutral hydrogen in the intergalactic medium (IGM) was ionized by the ultraviolet radiation emitted by these early sources. By investigating reionization, it is possible to gain insight into the formation and evolution of the first galaxies and black holes, as well as the feedback mechanisms that influenced subsequent galaxy evolution. Additionally, reionization provides essential information about the large-scale structure of the Universe, as the ionization bubbles created by galaxies trace the underlying cosmic web of matter distribution. Understanding reionization also helps interpret observations from contemporary and future telescopes, such as the James Webb Space Telescope (JWST) and the upcoming Square Kilometre Array (SKA), offering a clearer picture of the Universe's transition from the "Dark Ages" to the complex structures we observe today.

Acknowledgments

The authors acknowledge support from the Department of Atomic Energy, Government of India, under project no. 12-R&D-TFR-5.02-0700.

See Also: Barkana and Loeb (2001); Choudhury (2009); Loeb and Furlanetto (2013); Mesinger (2016); Dayal and Ferrara (2018); Choudhury (2022); Gnedin and Madau (2022)

References

- Abdurashidova Z, Aguirre JE, Alexander P, Ali ZS, Balfour Y, Beardsley AP, Bernardi G, Billings TS, Bowman JD, Bradley RF, Bull P, Burba J, Carey S, Carilli CL, Cheng C, DeBoer DR, Dexter M, de Lera Acedo E, Dibblee-Barkman T, Dillon JS, Ely J, Ewall-Wice A, Fagnoni N, Fritz R, Furlanetto SR, Gale-Sides K, Glendenning B, Gorghi D, Greig B, Grobbelaar J, Halday Z, Hazelton BJ, Hewitt JN, Hickish J, Jacobs DC, Julius A, Kern NS, Kerrigan J, Kittiwisit P, Kohn SA, Kolopanis M, Lanman A, La Plante P, Lekalake T, Lewis D, Liu A, MacMahon D, Malan L, Malgas C, Maree M, Martinot ZE, Matsetela E, Mesinger A, Molewa M, Morales MF, Mosiane T, Murray SG, Neben AR, Nikolic B, Nunhokee CD, Parsons AR, Patra N, Pascua R, Pieterse S, Pober JC, Razavi-Ghods N, Ringuette J, Robnett J, Rosie K, Sims P, Singh S, Smith C, Syce A, Thyagarajan N, Williams PKG, Zheng H and HERA Collaboration (2022), February. First Results from HERA Phase I: Upper Limits on the Epoch of Reionization 21 cm Power Spectrum. *ApJ* 925 (2), 221. doi:10.3847/1538-4357/ac1c78. 2108.02263.
- Álvarez-Márquez J, Colina L, Crespo Gómez A, Rinaldi P, Melinder J, Östlin G, Annunziatella M, Labiano A, Bik A, Bosman S, Greve TR, Wright G, Alonso-Herrero A, Boogaard L, Azollini R, Caputi KI, Costantini L, Eckart A, García-Marín M, Gillman S, Hjorth J, Iani E, Ilbert O, Jermann I, Langeroodi D, Meyer R, Peißker F, Pérez-González P, Pye JP, Tikkanen T, Topinka M, van der Werf P, Walter F, Henning T and Ray T (2024), Jun. Spatially resolved H α and ionizing photon production efficiency in the lensed galaxy MACS1149-JD1 at a redshift of 9.11. *A&A* 686, A85. doi:10.1051/0004-6361/202347946. 2309.06319.
- Anderson L, Governato F, Karcher M, Quinn T and Wadsley J (2017), Jul. The little Galaxies that could (reionize the universe): predicting faint end slopes & escape fractions at $z \lesssim 4$. *MNRAS* 468 (4): 4077–4092. doi:10.1093/mnras/stx709. 1606.05352.
- Atek H, Richard J, Kneib JP and Schaerer D (2018), Oct. The extreme faint end of the UV luminosity function at $z \sim 6$ through gravitational telescopes: a comprehensive assessment of strong lensing uncertainties. *MNRAS* 479 (4): 5184–5195. doi:10.1093/mnras/sty1820. 1803.09747.
- Atek H, Labbé I, Furtak LJ, Chemerynska I, Fujimoto S, Setton DJ, Miller TB, Oesch P, Bezanson R, Price SH, Dayal P, Zitrin A, Kokorev V, Weaver JR, Brammer G, Dokkum Pv, Williams CC, Cutler SE, Feldmann R, Fudamoto Y, Greene JE, Leja J, Maseda MV, Muzzin A, Pan R, Papovich C, Nelson EJ, Nanayakkara T, Stark DP, Stefanon M, Suess KA, Wang B and Whitaker KE (2024), Feb. Most of the photons that reionized the Universe came from dwarf galaxies. *Nature* 626 (8001): 975–978. doi:10.1038/s41586-024-07043-6.
- Barkana R and Loeb A (2001), Jul. In the beginning: the first sources of light and the reionization of the universe. *Phys. Rep.* 349 (2): 125–238. doi:10.1016/S0370-1573(01)00019-9. astro-ph/0010468.
- Barry N, Wilensky M, Trott CM, Pindor B, Beardsley AP, Hazelton BJ, Sullivan IS, Morales MF, Pober JC, Line J, Greig B, Byrne R, Lanman A, Li W, Jordan CH, Joseph RC, McKinley B, Rahimi M, Yoshiura S, Bowman JD, Gaensler BM, Hewitt JN, Jacobs DC, Mitchell DA, Udaya Shankar N, Sethi SK, Subrahmanyam R, Tingay SJ, Webster RL and Wyithe JSB (2019), October. Improving the Epoch of Reionization Power Spectrum Results from Murchison Widefield Array Season 1 Observations. *ApJ* 884 (1), 1. doi:10.3847/1538-4357/ab40a8. 1909.00561.
- Becker GD, Bolton JS, Madau P, Pettini M, Ryan-Weber EV and Venemans BP (2015), Mar. Evidence of patchy hydrogen reionization from an extreme Ly α trough below redshift six. *MNRAS* 447 (4): 3402–3419. doi:10.1093/mnras/stu2646. 1407.4850.
- Begley R, Cullen F, McLure RJ, Dunlop JS, Hall A, Carnall AC, Hamadouche ML, McLeod DJ, Amorín R, Calabrò A, Fontana A, Fynbo JPU, Guaita L, Hathi NP, Hibon P, Ji Z, Llerena M, Pentericci L, Saldana-Lopez A, Schaerer D, Talia M, Vanzella E and Zamorani G (2022), Jul.

- The VANDELS survey: a measurement of the average Lyman-continuum escape fraction of star-forming galaxies at $z = 3.5$. *MNRAS* 513 (3): 3510–3525. doi:10.1093/mnras/stac1067. 2202.04088.
- Begley R, McLure RJ, Cullen F, McLeod DJ, Dunlop JS, Carnall AC, Stanton TM, Shapley AE, Cochrane R, Donnan CT, Ellis RS, Fontana A, Grogan NA and Koekemoer AM (2025), Feb. The evolution of $[O\ III]+H\ \beta$ equivalent width from $z = 3 - 8$: implications for the production and escape of ionizing photons during reionization. *MNRAS* doi:10.1093/mnras/staf211. 2410.10988.
- Belikov AV and Hooper D (2009), Aug. How dark matter reionized the Universe. *Phys. Rev. D* 80 (3), 035007. doi:10.1103/PhysRevD.80.035007. 0904.1210.
- Beniamini P, Kumar P, Ma X and Quataert E (2021), Apr. Exploring the epoch of hydrogen reionization using FRBs. *MNRAS* 502 (4): 5134–5146. doi:10.1093/mnras/stab309. 2011.11643.
- Bolton JS and Haehnelt MG (2007), Jan. The nature and evolution of the highly ionized near-zones in the absorption spectra of $z \sim 6$ quasars. *MNRAS* 374 (2): 493–514. doi:10.1111/j.1365-2966.2006.11176.x. astro-ph/0607331.
- Bosman SEI, Fan X, Jiang L, Reed S, Matsuoka Y, Becker G and Haehnelt M (2018), Sep. New constraints on Lyman- α opacity with a sample of 62 quasars at $z \lesssim 5.7$. *MNRAS* 479 (1): 1055–1076. doi:10.1093/mnras/sty1344. 1802.08177.
- Bosman SEI, Davies FB, Becker GD, Keating LC, Davies RL, Zhu Y, Eilers AC, D’Odorico V, Bian F, Bischetti M, Cristiani SV, Fan X, Farina EP, Haehnelt MG, Hennawi JF, Kulkarni G, Mesinger A, Meyer RA, Onoue M, Pallottini A, Qin Y, Ryan-Weber E, Schindler JT, Walter F, Wang F and Yang J (2022), Jul. Hydrogen reionization ends by $z = 5.3$: Lyman- α optical depth measured by the XQR-30 sample. *MNRAS* 514 (1): 55–76. doi:10.1093/mnras/stac1046. 2108.03699.
- Boutsia K, Grazian A, Giallongo E, Fiore F and Civano F (2018), Dec. A High Space Density of L* Active Galactic Nuclei at $z \sim 4$ in the COSMOS Field. *ApJ* 869 (1), 20. doi:10.3847/1538-4357/aa6c7. 1811.06404.
- Bouwens RJ, Illingworth GD, Oesch PA, Trenti M, Labbé I, Bradley L, Carollo M, van Dokkum PG, Gonzalez V, Holwerda B, Franx M, Spitler L, Smit R and Magee D (2015), Apr. UV Luminosity Functions at Redshifts $z \sim 4$ to $z \sim 10$: 10,000 Galaxies from HST Legacy Fields. *ApJ* 803 (1), 34. doi:10.1088/0004-637X/803/1/34. 1403.4295.
- Bouwens RJ, Oesch PA, Illingworth GD, Ellis RS and Stefanon M (2017), Jul. The $z \sim 6$ Luminosity Function Fainter than -15 mag from the Hubble Frontier Fields: The Impact of Magnification Uncertainties. *ApJ* 843 (2), 129. doi:10.3847/1538-4357/aa70a4. 1610.00283.
- Bouwens R, Illingworth G, Oesch P, Stefanon M, Naidu R, van Leeuwen J and Magee D (2023), Jul. UV luminosity density results at $z \lesssim 8$ from the first JWST/NIRCam fields: limitations of early data sets and the need for spectroscopy. *MNRAS* 523 (1): 1009–1035. doi:10.1093/mnras/stad1014. 2212.06683.
- Bowler RAA, Jarvis MJ, Dunlop JS, McLure RJ, McLeod DJ, Adams NJ, Milvang-Jensen B and McCracken HJ (2020), Apr. A lack of evolution in the very bright end of the galaxy luminosity function from $z = 8$ to 10. *MNRAS* 493 (2): 2059–2084. doi:10.1093/mnras/staa313. 1911.12832.
- Bowman JD, Rogers AEE, Monsalve RA, Mozdzen TJ and Mahesh N (2018), Mar. An absorption profile centred at 78 megahertz in the sky-averaged spectrum. *Nature* 555 (7694): 67–70. doi:10.1038/nature25792. 1810.05912.
- Bunker AJ, Saxena A, Cameron AJ, Willott CJ, Curtis-Lake E, Jakobsen P, Carniani S, Smit R, Maiolino R, Witstok J, Curti M, D’Eugenio F, Jones GC, Ferruit P, Arribas S, Charlot S, Chevallard J, Giardino G, de Graaff A, Looser TJ, Lützgendorf N, Maseda MV, Rawle T, Rix HW, Del Pino BR, Alberts S, Egami E, Eisenstein DJ, Endsley R, Hainline K, Hausen R, Johnson BD, Rieke G, Rieke M, Robertson BE, Shivaee I, Stark DP, Sun F, Tacchella S, Tang M, Williams CC, Willmer CNA, Baker WM, Baum S, Bhatawdekar R, Bowler R, Boyett K, Chen Z, Circosta C, Helton JM, Ji Z, Kumari N, Lyu J, Nelson E, Parlanti E, Perna M, Sandles L, Scholtz J, Suess KA, Topping MW, Übler H, Wallace IEB and Whittler L (2023), Sep. JADES NIRSpec Spectroscopy of GN-z11: Lyman- α emission and possible enhanced nitrogen abundance in a $z = 10.60$ luminous galaxy. *A&A* 677, A88. doi:10.1051/0004-6361/202346159. 2302.07256.
- Calabro A, Castellano M, Zavala JA, Pentericci L, Arrabal Haro P, Bakx TJLC, Burgarella D, Casey CM, Dickinson M, Finkelstein SL, Fontana A, Llerena M, Mascia S, Merlin E, Mitsuhashi I, Napolitano L, Paris D, Perez-Gonzalez PG, Roberts-Borsani G, Santini P, Treu T and Vanzella E (2024), Mar. Evidence of extreme ionization conditions and low metallicity in GHZ2/GLASS-z12 from a combined analysis of NIRSpec and MIRI observations. *arXiv e-prints*, arXiv:2403.12683doi:10.48550/arXiv.2403.12683. 2403.12683.
- Carilli CL, Wang R, Fan X, Walter F, Kurk J, Riechers D, Wagg J, Hennawi J, Jiang L, Menten KM, Bertoldi F, Strauss MA and Cox P (2010), May. Ionization Near Zones Associated with Quasars at $z \sim 6$. *ApJ* 714 (1): 834–839. doi:10.1088/0004-637X/714/1/834. 1003.0016.
- Chakraborty A and Choudhury TR (2024), Jul. Modelling the star-formation activity and ionizing properties of high-redshift galaxies. *J. Cosmology Astropart. Phys.* 2024 (7), 078. doi:10.1088/1475-7516/2024/07/078. 2404.02879.
- Chardin J, Puchwein E and Haehnelt MG (2017), Mar. Large-scale opacity fluctuations in the Ly α forest: evidence for QSOs dominating the ionizing UV background at $z \sim 5.5$ – 6.7 . *MNRAS* 465 (3): 3429–3445. doi:10.1093/mnras/stw2943. 1606.08231.
- Chatterjee A, Choudhury TR and Mitra S (2021), Oct. CosmoReionMC: a package for estimating cosmological and astrophysical parameters using CMB, Lyman- α absorption, and global 21 cm data. *MNRAS* 507 (2): 2405–2422. doi:10.1093/mnras/stab2316. 2101.11088.
- Chisholm J, Saldana-Lopez A, Flury S, Schaerer D, Jaskot A, Amorin R, Atek H, Finkelstein SL, Fleming B, Ferguson H, Fernández V, Giallisco M, Hayes M, Heckman T, Henry A, Ji Z, Marques-Chaves R, Mauerhofer V, McCandliss S, Oey MS, Ostlin G, Rutkowski M, Scarlata C, Thuan T, Trebitsch M, Wang B, Worseck G and Xu X (2022), Dec. The far-ultraviolet continuum slope as a Lyman Continuum escape estimator at high redshift. *MNRAS* 517 (4): 5104–5120. doi:10.1093/mnras/stac2874. 2207.05771.
- Choudhury TR (2009), Sep. Analytical Models of the Intergalactic Medium and Reionization. *Current Science* 97: 841. doi:10.48550/arXiv.0904.4596. 0904.4596.
- Choudhury TR (2022), Sep. A short introduction to reionization physics. *General Relativity and Gravitation* 54 (9), 102. doi:10.1007/s10714-022-02987-4. 2209.08558.
- Choudhury TR and Paranjape A (2018), Dec. Photon number conservation and the large-scale 21 cm power spectrum in seminumerical models of reionization. *MNRAS* 481 (3): 3821–3837. doi:10.1093/mnras/sty2551. 1807.00836.
- Choudhury TR, Haehnelt MG and Regan J (2009), Apr. Inside-out or outside-in: the topology of reionization in the photon-starved regime suggested by Ly α forest data. *MNRAS* 394 (2): 960–977. doi:10.1111/j.1365-2966.2008.14383.x. 0806.1524.
- Choustikov N, Katz H, Saxena A, Cameron AJ, Devriendt J, Slyz A, Rosdahl J, Blaizot J and Michel-Dansac L (2024), Apr. The Physics of Indirect Estimators of Lyman Continuum Escape and their Application to High-Redshift JWST Galaxies. *MNRAS* 529 (4): 3751–3767. doi:10.1093/mnras/stae776. 2304.08526.
- Curtis-Lake E, Carniani S, Cameron A, Charlot S, Jakobsen P, Maiolino R, Bunker A, Witstok J, Smit R, Chevallard J, Willott C, Ferruit P, Arribas S, Bonaventura N, Curti M, D’Eugenio F, Franx M, Giardino G, Looser TJ, Lützgendorf N, Maseda MV, Rawle T, Rix HW, Rodríguez del Pino B, Übler H, Sirianni M, Dressler A, Egami E, Eisenstein DJ, Endsley R, Hainline K, Hausen R, Johnson BD, Rieke M, Robertson B, Shivaee I, Stark DP, Tacchella S, Williams CC, Willmer CNA, Bhatawdekar R, Bowler R, Boyett K, Chen Z, de Graaff A, Helton JM, Hviding RE, Jones GC, Kumari N, Lyu J, Nelson E, Perna M, Sandles L, Saxena A, Suess KA, Sun F, Topping MW, Wallace IEB and Whittler L (2023), May. Spectroscopic confirmation of four metal-poor galaxies at $z = 10.3$ – 13.2 . *Nature Astronomy* 7: 622–632. doi:10.1038/s41550-023-01918-w. 2212.04568.
- D’Aloisio A, McQuinn M and Trac H (2015), Nov. Large Opacity Variations in the High-redshift Ly α Forest: The Signature of Relic Temperature

- Fluctuations from Patchy Reionization. *ApJ* 813 (2), L38. doi:10.1088/2041-8205/813/2/L38. 1509.02523.
- Davies FB and Furlanetto SR (2016), Aug. Large fluctuations in the hydrogen-ionizing background and mean free path following the epoch of reionization. *MNRAS* 460 (2): 1328–1339. doi:10.1093/mnras/stw931. 1509.07131.
- Dayal P and Ferrara A (2018), Dec. Early galaxy formation and its large-scale effects. *Phys. Rep.* 780: 1–64. doi:10.1016/j.physrep.2018.10.002. 1809.09136.
- de Lera Acedo E, de Villiers DIL, Razavi-Ghods N, Handley W, Fialkov A, Magro A, Anstey D, Bevins HTJ, Chiello R, Cumner J, Josaitis AT, Roque ILV, Sims PH, Scheutwinkel KH, Alexander P, Bernardi G, Carey S, Cavillot J, Croukamp W, Ely JA, Gessey-Jones T, Gueuning Q, Hills R, Kulkarni G, Maiolino R, Meerburg PD, Mittal S, Pritchard JR, Puchwein E, Saxena A, Shen E, Smirnov O, Spinelli M and Zarb-Adami K (2022), Jul. The REACH radiometer for detecting the 21-cm hydrogen signal from redshift $z \approx 7.5$ –28. *Nature Astronomy* 6: 984–998. doi:10.1038/s41550-022-01709-9. 2210.07409.
- Dijkstra M (2014), Oct. Ly α Emitting Galaxies as a Probe of Reionisation. *PASA* 31, e040. doi:10.1017/pasa.2014.33. 1406.7292.
- Donnan CT, McLeod DJ, Dunlop JS, McLure RJ, Carnall AC, Begley R, Cullen F, Hamadouche ML, Bowler RAA, Magee D, McCracken HJ, Milvang-Jensen B, Moneti A and Targett T (2023), Feb. The evolution of the galaxy UV luminosity function at redshifts $z = 8$ –15 from deep JWST and ground-based near-infrared imaging. *MNRAS* 518 (4): 6011–6040. doi:10.1093/mnras/stac3472. 2207.12356.
- Donnan CT, McLure RJ, Dunlop JS, McLeod DJ, Magee D, Arellano-Córdova KZ, Barrufet L, Begley R, Bowler RAA, Carnall AC, Cullen F, Ellis RS, Fontana A, Illingworth GD, Grogin NA, Hamadouche ML, Koekemoer AM, Liu FY, Mason C, Santini P and Stanton TM (2024), Sep. JWST PRIMER: a new multifield determination of the evolving galaxy UV luminosity function at redshifts $z = 9$ –15. *MNRAS* 533 (3): 3222–3237. doi:10.1093/mnras/stac2037. 2403.03171.
- Endsley R and Stark DP (2022), Apr. Strong Lyman- α emission in an overdense region at $z = 6.8$: a very large (R 3 physical Mpc) ionized bubble in COSMOS? *MNRAS* 511 (4): 6042–6054. doi:10.1093/mnras/stac524. 2112.14779.
- Endsley R, Stark DP, Whittler B, Topping MW, Johnson BD, Robertson B, Tacchella S, Alberts S, Baker WM, Bhatawdekar R, Boyett K, Bunker AJ, Cameron AJ, Carniani S, Charlot S, Chen Z, Chevillard J, Curtis-Lake E, Danhaive AL, Egami E, Eisenstein DJ, Hainline K, Helton JM, Ji Z, Looser TJ, Maiolino R, Nelson E, Puskás D, Rieke G, Rieke M, Rix HW, Sandles L, Saxena A, Simmonds C, Smit R, Sun F, Williams CC, Willmer CNA, Willott C and Witstok J (2023), Jun. The Star-forming and Ionizing Properties of Dwarf $z=6$ –9 Galaxies in JADES: Insights on Bursty Star Formation and Ionized Bubble Growth. *arXiv e-prints*, arXiv:2306.05295doi:10.48550/arXiv.2306.05295. 2306.05295.
- Fan X, Strauss MA, Becker RH, White RL, Gunn JE, Knapp GR, Richards GT, Schneider DP, Brinkmann J and Fukugita M (2006), Jul. Constraining the Evolution of the Ionizing Background and the Epoch of Reionization with $z=6$ Quasars. II. A Sample of 19 Quasars. *AJ* 132 (1): 117–136. doi:10.1086/504836. astro-ph/0512082.
- Fialkov A and Loeb A (2016), May. Constraining the CMB optical depth through the dispersion measure of cosmological radio transients. *J. Cosmology Astropart. Phys.* 2016 (5), 004. doi:10.1088/1475-7516/2016/05/004. 1602.08130.
- Flury SR, Jaskot AE, Ferguson HC, Worseck G, Makan K, Chisholm J, Saldana-Lopez A, Schaefer D, McCandliss S, Wang B, Ford NM, Heckman T, Ji Z, Giallisco M, Amorin R, Atek H, Blaizot J, Borthakur S, Carr C, Castellano M, Cristiani S, De Barros S, Dickinson M, Finkelstein SL, Fleming B, Fontanot F, Garel T, Grazian A, Hayes M, Henry A, Mauerhofer V, Micheva G, Oey MS, Ostlin G, Papovich C, Pentericci L, Ravindranath S, Rosdahl J, Rutkowski M, Santini P, Scarlata C, Teplitz H, Thuan T, Trebitsch M, Vanzella E, Verhamme A and Xu X (2022), May. The Low-redshift Lyman Continuum Survey. I. New, Diverse Local Lyman Continuum Emitters. *ApJS* 260 (1), 1. doi:10.3847/1538-4365/ac5331. 2201.11716.
- Furlanetto SR, Zaldarriaga M and Hernquist L (2004), Sep. The Growth of H II Regions During Reionization. *ApJ* 613 (1): 1–15. doi:10.1086/423025. astro-ph/0403697.
- Gaikwad P, Rauch M, Haehnelt MG, Puchwein E, Bolton JS, Keating LC, Kulkarni G, Iršič V, Bañados E, Becker GD, Boera E, Zahedy FS, Chen HW, Carswell RF, Chardin J and Rorai A (2020), Jun. Probing the thermal state of the intergalactic medium at $z \lesssim 6$ with the transmission spikes in high-resolution Ly α forest spectra. *MNRAS* 494 (4): 5091–5109. doi:10.1093/mnras/staa907. 2001.10018.
- Gaikwad P, Haehnelt MG, Davies FB, Bosman SEI, Molaro M, Kulkarni G, D’Odorico V, Becker GD, Davies RL, Nasir F, Bolton JS, Keating LC, Iršič V, Puchwein E, Zhu Y, Asthana S, Yang J, Lai S and Eilers AC (2023), Nov. Measuring the photoionization rate, neutral fraction, and mean free path of H I ionizing photons at $4.9 \leq z \leq 6.0$ from a large sample of XShooter and ESI spectra. *MNRAS* 525 (3): 4093–4120. doi:10.1093/mnras/stad2566. 2304.02038.
- Gallerani S, Choudhury TR and Ferrara A (2006), Aug. Constraining the reionization history with QSO absorption spectra. *MNRAS* 370 (3): 1401–1421. doi:10.1111/j.1365-2966.2006.10553.x. astro-ph/0512129.
- Gallerani S, Ferrara A, Fan X and Choudhury TR (2008), May. Glimpsing through the high-redshift neutral hydrogen fog. *MNRAS* 386 (1): 359–369. doi:10.1111/j.1365-2966.2008.13029.x. 0706.1053.
- Gehlot BK, Mertens FG, Koopmans LVE, Brentjens MA, Zaroubi S, Ciardi B, Ghosh A, Hatem M, Iliev IT, Jelić V, Kooistra R, Krause F, Mellema G, Mevius M, Mitra M, Offringa AR, Pandey VN, Sardarabadi AM, Schaye J, Silva MB, Vedantham HK and Yatawatta S (2019), September. The first power spectrum limit on the 21-cm signal of neutral hydrogen during the Cosmic Dawn at $z = 20$ –25 from LOFAR. *MNRAS* 488 (3): 4271–4287. doi:10.1093/mnras/stz1937. 1809.06661.
- Giallongo E, Grazian A, Fiore F, Kodra D, Urrutia T, Castellano M, Cristiani S, Dickinson M, Fontana A, Menci N, Pentericci L, Boutsia K, Newman JA and Puccetti S (2019), Oct. Space Densities and Emissivities of Active Galactic Nuclei at $z \lesssim 4$. *ApJ* 884 (1), 19. doi:10.3847/1538-4357/ab39e1.
- Gnedin NY and Madau P (2022), Dec. Modeling cosmic reionization. *Living Reviews in Computational Astrophysics* 8 (1), 3. doi:10.1007/s41115-022-00015-5. 2208.02260.
- Gorce A, Ilić S, Douspis M, Aubert D and Langer M (2020), Aug. Improved constraints on reionisation from CMB observations: A parameterisation of the kSZ effect. *A&A* 640, A90. doi:10.1051/0004-6361/202038170. 2004.06616.
- Goto H, Shimasaku K, Yamanaka S, Momose R, Ando M, Harikane Y, Hashimoto T, Inoue AK and Ouchi M (2021), Dec. SILVERRUSH. XI. Constraints on the Ly α Luminosity Function and Cosmic Reionization at $z = 7.3$ with Subaru/Hyper Suprime-Cam. *ApJ* 923 (2), 229. doi:10.3847/1538-4357/ac308b. 2110.14474.
- Grazian A, Giallongo E, Boutsia K, Cristiani S, Vanzella E, Scarlata C, Santini P, Pentericci L, Merlin E, Menci N, Fontanot F, Fontana A, Fiore F, Civano F, Castellano M, Brusa M, Bonchi A, Carini R, Cusano F, Faccini M, Garilli B, Marchetti A, Rossi A and Speziali R (2018), May. The contribution of faint AGNs to the ionizing background at $z < 4$. *A&A* 613, A44. doi:10.1051/0004-6361/201732385. 1802.01953.
- Gunn JE and Peterson BA (1965), Nov. On the Density of Neutral Hydrogen in Intergalactic Space. *ApJ* 142: 1633–1636. doi:10.1086/148444.
- Harikane Y, Ono Y, Ouchi M, Liu C, Sawicki M, Shibuya T, Behroozi PS, He W, Shimasaku K, Arnouts S, Coupon J, Fujimoto S, Gwyn S, Huang J, Inoue AK, Kashikawa N, Komiyama Y, Matsuoka Y and Willott CJ (2022), Mar. GOLDRUSH. IV. Luminosity Functions and Clustering Revealed with 4,000,000 Galaxies at $z=2$ –7: Galaxy-AGN Transition, Star Formation Efficiency, and Implication for Evolution at $z \lesssim 10$. *ApJS* 259 (1), 20. doi:10.3847/1538-4365/ac3dfc. 2108.01090.
- Harikane Y, Ouchi M, Oguri M, Ono Y, Nakajima K, Isobe Y, Umeda H, Mawatari K and Zhang Y (2023a), Mar. A Comprehensive Study of Galaxies at $z=9$ –16 Found in the Early JWST Data: Ultraviolet Luminosity Functions and Cosmic Star Formation History at the Pre-reionization

- Epoch. *ApJS* 265 (1), 5. doi:10.3847/1538-4365/aca9. 2208.01612.
- Harikane Y, Zhang Y, Nakajima K, Ouchi M, Isobe Y, Ono Y, Hatano S, Xu Y and Umeda H (2023b), Dec. A JWST/NIRSpec First Census of Broad-line AGNs at $z = 4-7$: Detection of 10 Faint AGNs with $M_{BH} 10^6-10^8 M_{\odot}$ and Their Host Galaxy Properties. *ApJ* 959 (1), 39. doi:10.3847/1538-4357/ad029e. 2303.11946.
- Hazra DK and Smoot GF (2017), Nov. Witnessing the reionization history using Cosmic Microwave Background observation from Planck. *J. Cosmology Astropart. Phys.* 2017 (11), 028. doi:10.1088/1475-7516/2017/11/028. 1708.04913.
- Heimersheim S, Sartorio NS, Fialkov A and Lorimer DR (2022), Jul. What It Takes to Measure Reionization with Fast Radio Bursts. *ApJ* 933 (1), 57. doi:10.3847/1538-4357/ac70c9. 2107.14242.
- Hutter A (2018), Jun. The accuracy of seminumerical reionization models in comparison with radiative transfer simulations. *MNRAS* 477 (2): 1549–1566. doi:10.1093/mnras/sty683. 1803.00088.
- Hutter A, Heneka C, Dayal P, Gottlöber S, Mesinger A, Trebitsch M and Yepes G (2023), Oct. On the general nature of 21-cm-Lyman α emitter cross-correlations during reionization. *MNRAS* 525 (2): 1664–1676. doi:10.1093/mnras/stad2376. 2306.03156.
- Itoh R, Ouchi M, Zhang H, Inoue AK, Mawatari K, Shibuya T, Harikane Y, Ono Y, Kusakabe H, Shimasaku K, Fujimoto S, Iwata I, Kajisawa M, Kashikawa N, Kawanamoto S, Komiyama Y, Lee CH, Nagao T and Taniguchi Y (2018), Nov. CHORUS. II. Subaru/HSC Determination of the Ly α Luminosity Function at $z = 7.0$: Constraints on Cosmic Reionization Model Parameter. *ApJ* 867 (1), 46. doi:10.3847/1538-4357/aadfe4. 1805.05944.
- Izotov YI, Worseck G, Schaerer D, Guseva NG, Thuan TX, Fricke Verhamme A and Orlitová I (2018), Aug. Low-redshift Lyman continuum leaking galaxies with high [O III]/[O II] ratios. *MNRAS* 478 (4): 4851–4865. doi:10.1093/mnras/sty1378. 1805.09865.
- Izotov YI, Worseck G, Schaerer D, Guseva NG, Chisholm J, Thuan TX, Fricke KJ and Verhamme A (2021), May. Lyman continuum leakage from low-mass galaxies with $M_{*} \geq 10^8 M_{\odot}$. *MNRAS* 503 (2): 1734–1752. doi:10.1093/mnras/stab612. 2103.01514.
- Jain D, Choudhury TR, Raghunathan S and Mukherjee S (2024), May. Probing the physics of reionization using kinematic Sunyaev-Zeldovich power spectrum from current and upcoming cosmic microwave background surveys. *MNRAS* 530 (1): 35–51. doi:10.1093/mnras/stae748. 2311.00315.
- Jaskot AE and Oey MS (2013), Apr. The Origin and Optical Depth of Ionizing Radiation in the “Green Pea” Galaxies. *ApJ* 766 (2), 91. doi:10.1088/0004-637X/766/2/91. 1301.0530.
- Jin X, Yang J, Fan X, Wang F, Bañados E, Bian F, Davies FB, Eilers AC, Farina EP, Hennawi JF, Pacucci F, Venemans B and Walter F (2023), Jan. (Nearly) Model-independent Constraints on the Neutral Hydrogen Fraction in the Intergalactic Medium at $z = 5-7$ Using Dark Pixel Fractions in Ly α and Ly β Forests. *ApJ* 942 (2), 59. doi:10.3847/1538-4357/aca678. 2211.12613.
- Jones GC, Bunker AJ, Saxena A, Arribas S, Bhatawdekar R, Boyett K, Carniani S, Charlot S, Curtis-Lake E, Hainline K, Johnson BD, Kumari N, Maseda MV, Rix HW, Robertson BE, Tacchella S, Übler H, Williams CC, Willott C, Witstok J and Zhu Y (2024), Sep. JADES: Measuring reionization properties using Lyman-alpha emission. *arXiv e-prints*, arXiv:2409.06405doi:10.48550/arXiv.2409.06405. 2409.06405.
- Joshi N and Sharma M (2024), Mar. The haloes that reionized the Universe. *arXiv e-prints*, arXiv:2403.12132doi:10.48550/arXiv.2403.12132. 2403.12132.
- Kolopanis M, Jacobs DC, Cheng C, Parsons AR, Kohn SA, Pober JC, Aguirre JE, Ali ZS, Bernardi G, Bradley RF, Carilli CL, DeBoer DR, Dexter MR, Dillon JS, Kerrigan J, Klima P, Liu A, MacMahon DHE, Moore DF, Thyagarajan N, Nunhokee CD, Walbrough WP and Walker A (2019), Oct. A Simplified, Lossless Reanalysis of PAPER-64. *ApJ* 883 (2), 133. doi:10.3847/1538-4357/ab3e3a. 1909.02085.
- Konno A, Ouchi M, Shibuya T, Ono Y, Shimasaku K, Taniguchi Y, Nagao T, Kobayashi MAR, Kajisawa M, Kashikawa N, Inoue AK, Oguri M, Furusawa H, Goto T, Harikane Y, Higuchi R, Komiyama Y, Kusakabe H, Miyazaki S, Nakajima K and Wang SY (2018), Jan. SILVERRUSH. IV. Ly α luminosity functions at $z = 5.7$ and 6.6 studied with ~ 1300 Ly α emitters on the $14-21 \text{ deg}^2$ sky. *PASJ* 70, S16. doi:10.1093/pasj/psx131. 1705.01222.
- Koopmans L, Pritchard J, Mellema G, Aguirre J, Ahn K, Barkana R, van Bemmell I, Bernardi G, Bonaldi A, Briggs F, de Bruyn AG, Chang TC, Chapman E, Chen X, Ciardi B, Dayal P, Ferrara A, Fialkov A, Fiore F, Ichiki K, Illiev IT, Inoue S, Jelic V, Jones M, Lazio J, Maio U, Majumdar S, Mack KJ, Mesinger A, Morales MF, Parsons A, Pen UL, Santos M, Schneider R, Semelin B, de Souza RS, Subrahmanyan R, Takeuchi T, Vedantham H, Wagg J, Webster R, Wyithe S, Datta KK and Trott C (2015), April, The Cosmic Dawn and Epoch of Reionisation with SKA, Advancing Astrophysics with the Square Kilometre Array (AASKA14), pp. 1, 1505.07568.
- Kulkarni G, Keating LC, Haehnelt MG, Bosman SEI, Puchwein E, Chardin J and Aubert D (2019a), May. Large Ly α opacity fluctuations and low CMB τ in models of late reionization with large islands of neutral hydrogen extending to $z \geq 5.5$. *MNRAS* 485 (1): L24–L28. doi:10.1093/mnras/slz025. 1809.06374.
- Kulkarni G, Worseck G and Hennawi JF (2019b), Sep. Evolution of the AGN UV luminosity function from redshift 7.5. *MNRAS* 488 (1): 1035–1065. doi:10.1093/mnras/stz1493. 1807.09774.
- Lewis JSW, Ocvirk P, Aubert D, Sorce JG, Shapiro PR, Deparis N, Dawoodbhoy T, Teysier R, Yepes G, Gottlöber S, Ahn K, Illiev IT and Chardin J (2020), Aug. Galactic ionizing photon budget during the epoch of reionization in the Cosmic Dawn II simulation. *MNRAS* 496 (4): 4342–4357. doi:10.1093/mnras/staa1748. 2001.07785.
- Lidz A, Zahn O, Furlanetto SR, McQuinn M, Hernquist L and Zaldarriaga M (2009), Jan. Probing Reionization with the 21 cm Galaxy Cross-Power Spectrum. *ApJ* 690 (1): 252–266. doi:10.1088/0004-637X/690/1/252. 0806.1055.
- Liu H, Slatyer TR and Zavala J (2016), Sep. Contributions to cosmic reionization from dark matter annihilation and decay. *Phys. Rev. D* 94 (6), 063507. doi:10.1103/PhysRevD.94.063507. 1604.02457.
- Liu P, Ma Q, Han Y and Luo R (2024), May. A quantification of the effects using different stellar population synthesis models for epoch of reionization. *arXiv e-prints*, arXiv:2405.01821doi:10.48550/arXiv.2405.01821. 2405.01821.
- Loeb A and Furlanetto SR (2013). *The First Galaxies in the Universe*, stu - student edition ed., Princeton University Press. ISBN 9780691144917. <http://www.jstor.org/stable/j.ctt24hrpv>.
- Ma X, Quataert E, Wetzel A, Faucher-Giguère CA and Boylan-Kolchin M (2021), Jul. The contribution of globular clusters to cosmic reionization. *MNRAS* 504 (3): 4062–4071. doi:10.1093/mnras/stab1132. 2006.10065.
- Madau P, Haardt F and Rees MJ (1999), Apr. Radiative Transfer in a Clumpy Universe. III. The Nature of Cosmological Ionizing Sources. *ApJ* 514 (2): 648–659. doi:10.1086/306975. astro-ph/9809058.
- Madau P, Rees MJ, Volonteri M, Haardt F and Oh SP (2004), Apr. Early Reionization by Mini-quasars. *ApJ* 604 (2): 484–494. doi:10.1086/381935. astro-ph/0310223.
- Madau P, Giallongo E, Grazian A and Haardt F (2024), Aug. Cosmic Reionization in the JWST Era: Back to AGNs? *ApJ* 971 (1), 75. doi:10.3847/1538-4357/ad5ce8. 2406.18697.
- Maiolino R, Scholtz J, Curtis-Lake E, Carniani S, Baker W, de Graaff A, Tacchella S, Übler H, D’Eugenio F, Witstok J, Curti M, Arribas S, Bunker AJ, Charlot S, Chevillard J, Eisenstein DJ, Egami E, Ji Z, Jones GC, Lyu J, Rawle T, Robertson B, Rujopakarn W, Perna M, Sun F, Venturi G, Williams CC and Willott C (2023), Aug. JADES. The diverse population of infant Black Holes at $4 < z < 11$: merging, tiny, poor, but mighty. *arXiv e-prints*, arXiv:2308.01230doi:10.48550/arXiv.2308.01230. 2308.01230.

- Maity B (2024), Sep. Prospects of fast radio bursts and large-scale 21 cm power spectra in constraining the Epoch of Reionization. *A&A* 689, A340. doi:10.1051/0004-6361/202451160. 2408.05722.
- Maity B and Choudhury TR (2022), Sep. Constraining the reionization and thermal history of the Universe using a seminumerical photon-conserving code SCRIPT. *MNRAS* 515 (1): 617–630. doi:10.1093/mnras/stac1847. 2204.05268.
- Mapelli M, Ferrara A and Pierpaoli E (2006), Jul. Impact of dark matter decays and annihilations on reionization. *MNRAS* 369 (4): 1719–1724. doi:10.1111/j.1365-2966.2006.10408.x. astro-ph/0603237.
- Matthee J, Mackenzie R, Simcoe RA, Kashino D, Lilly SJ, Bordoloi R and Eilers AC (2023), Jun. EIGER. II. First Spectroscopic Characterization of the Young Stars and Ionized Gas Associated with Strong H β and [O III] Line Emission in Galaxies at $z = 5-7$ with JWST. *ApJ* 950 (1), 67. doi:10.3847/1538-4357/acc846. 2211.08255.
- Matthee J, Naidu RP, Brammer G, Chisholm J, Eilers AC, Goulding A, Greene J, Kashino D, Labbe I, Lilly SJ, Mackenzie R, Oesch PA, Weibel A, Wuyts S, Xiao M, Bordoloi R, Bouwens R, van Dokkum P, Illingworth G, Kramarenko I, Maseda MV, Mason C, Meyer RA, Nelson EJ, Reddy NA, Shivaei I, Simcoe RA and Yue M (2024), Mar. Little Red Dots: An Abundant Population of Faint Active Galactic Nuclei at $z \sim 5$ Revealed by the EIGER and FRESCO JWST Surveys. *ApJ* 963 (2), 129. doi:10.3847/1538-4357/ad2345. 2306.05448.
- McGreer ID, Mesinger A and D'Odorico V (2015), Feb. Model-independent evidence in favour of an end to reionization by $z \approx 6$. *MNRAS* 447 (1): 499–505. doi:10.1093/mnras/stu2449. 1411.5375.
- McLeod DJ, Donnan CT, McLure RJ, Dunlop JS, Magee D, Begley R, Carnall AC, Cullen F, Ellis RS, Hamadouche ML and Stanton TM (2024), Jan. The galaxy UV luminosity function at $z \approx 11$ from a suite of public JWST ERS, ERO, and Cycle-1 programs. *MNRAS* 527 (3): 5004–5022. doi:10.1093/mnras/stad3471. 2304.14469.
- Mertens FG, Mevius M, Koopmans LVE, Offringa AR, Mellema G, Zaroubi S, Brentjens MA, Gan H, Gehlot BK, Pandey VN, Sardarabadi AM, Vedantham HK, Yatawatta S, Asad KMB, Ciardi B, Chapman E, Gazagnes S, Ghara R, Ghosh A, Giri SK, Iliev IT, Jelić V, Kooistra R, Mondal R, Schaye J and Silva MB (2020), April. Improved upper limits on the 21 cm signal power spectrum of neutral hydrogen at $z \approx 9.1$ from LOFAR. *MNRAS* 493 (2): 1662–1685. doi:10.1093/mnras/staa327. 2002.07196.
- Mesinger A, (Ed.) (2016), Jan. Understanding the Epoch of Cosmic Reionization, Astrophysics and Space Science Library, 423. doi:10.1007/978-3-319-21957-8.
- Mesinger A and Furlanetto S (2007), Nov. Efficient Simulations of Early Structure Formation and Reionization. *ApJ* 669 (2): 663–675. doi:10.1086/521806. 0704.0946.
- Mesinger A, Furlanetto S and Cen R (2011), Feb. 21CMFAST: a fast, seminumerical simulation of the high-redshift 21-cm signal. *MNRAS* 411 (2): 955–972. doi:10.1111/j.1365-2966.2010.17731.x. 1003.3878.
- Mirabel IF, Dijkstra M, Laurent P, Loeb A and Pritchard JR (2011), Apr. Stellar black holes at the dawn of the universe. *A&A* 528, A149. doi:10.1051/0004-6361/201016357. 1102.1891.
- Miranda V, Lidz A, Heinrich CH and Hu W (2017), Jun. CMB signatures of metal-free star formation and Planck 2015 polarization data. *MNRAS* 467 (4): 4050–4056. doi:10.1093/mnras/stx306. 1610.00691.
- Mondal R, Bharadwaj S and Majumdar S (2021), Jul. ReionYuga: Epoch of Reionization neutral Hydrogen field generator. Astrophysics Source Code Library, record ascl:2107.005.
- Naidu RP, Tacchella S, Mason CA, Bose S, Oesch PA and Conroy C (2020), Apr. Rapid Reionization by the Oligarchs: The Case for Massive, UV-bright, Star-forming Galaxies with High Escape Fractions. *ApJ* 892 (2), 109. doi:10.3847/1538-4357/ab7cc9. 1907.13130.
- Nakajima K and Ouchi M (2014), Jul. Ionization state of inter-stellar medium in galaxies: evolution, SFR- M_* - Z dependence, and ionizing photon escape. *MNRAS* 442 (1): 900–916. doi:10.1093/mnras/stu902. 1309.0207.
- Nasir F and D'Aloisio A (2020), May. Observing the tail of reionization: neutral islands in the $z = 5.5$ Lyman- α forest. *MNRAS* 494 (3): 3080–3094. doi:10.1093/mnras/staa894. 1910.03570.
- Nikolić I, Mesinger A, Qin Y and Gorce A (2023), Dec. Inferring reionization and galaxy properties from the patchy kinetic Sunyaev-Zel'dovich signal. *MNRAS* 526 (2): 3170–3183. doi:10.1093/mnras/stad2961. 2307.01265.
- Ono Y, Ouchi M, Harikane Y, Toshikawa J, Rauch M, Yuma S, Sawicki M, Shibuya T, Shimasaku K, Oguri M, Willott C, Akhlaghi M, Akiyama M, Coupon J, Kashikawa N, Komiyama Y, Konno A, Lin L, Matsuoka Y, Miyazaki S, Nagao T, Nakajima K, Silverman J, Tanaka M, Taniguchi Y and Wang SY (2018), Jan. Great Optically Luminous Dropout Research Using Subaru HSC (GOLDRUSH). I. UV luminosity functions at $z \sim 4-7$ derived with the half-million dropouts on the 100 deg 2 sky. *PAJ* 70, S10. doi:10.1093/pasj/psx103. 1704.06004.
- Ouchi M, Ono Y and Shibuya T (2020), Aug. Observations of the Lyman- α Universe. *ARA&A* 58: 617–659. doi:10.1146/annurev-astro-032620-021859. 2012.07960.
- Pahl AJ, Shapley A, Steidel CC, Chen Y and Reddy NA (2021), Aug. An uncontaminated measurement of the escaping Lyman continuum at $z = 3$. *MNRAS* 505 (2): 2447–2467. doi:10.1093/mnras/stab1374. 2104.02081.
- Paoletti D, Hazra DK, Finelli F and Smoot GF (2024), May. The asymmetry of dawn: evidence for asymmetric reionization histories from a joint analysis of cosmic microwave background and astrophysical data. *arXiv e-prints*, arXiv:2405.09506doi:10.48550/arXiv.2405.09506. 2405.09506.
- Park H, Shapiro PR, Komatsu E, Iliev IT, Ahn K and Mellema G (2013), Jun. The Kinetic Sunyaev-Zel'dovich Effect as a Probe of the Physics of Cosmic Reionization: The Effect of Self-regulated Reionization. *ApJ* 769 (2), 93. doi:10.1088/0004-637X/769/2/93. 1301.3607.
- Parsons AR, Backer DC, Foster GS, Wright MCH, Bradley RF, Gugliucci NE, Parashare CR, Benoit EE, Aguirre JE, Jacobs DC, Carilli CL, Herne D, Lynch MJ, Manley JR and Werthimer DJ (2010), April. The Precision Array for Probing the Epoch of Re-ionization: Eight Station Results. *AJ* 139 (4): 1468–1480. doi:10.1088/0004-6256/139/4/1468. 0904.2334.
- Paul S, Mukherjee S and Choudhury TR (2021), Jan. Inevitable imprints of patchy reionization on the cosmic microwave background anisotropy. *MNRAS* 500 (1): 232–246. doi:10.1093/mnras/staa3221. 2005.05327.
- Planck Collaboration, Aghanim N, Akrami Y, Ashdown M, Aumont J, Baccigalupi C, Ballardini M, Banday AJ, Barreiro RB, Bartolo N, Basak S, Battye R, Benabed K, Bernard JP, Bersanelli M, Bielewicz P, Bock JJ, Bond JR, Borrill J, Bouchet FR, Boulanger F, Bucher M, Burigana C, Butler RC, Calabrese E, Cardoso JF, Carron J, Challinor A, Chiang HC, Chluba J, Colombo LPL, Combet C, Contreras D, Crill BP, Cuttaia F, de Bernardis P, de Zotti G, Delabrouille J, Delouis JM, Di Valentino E, Diego JM, Doré O, Douspis M, Ducout A, Dupac X, Dusini S, Efstathiou G, Elsner F, Enßlin TA, Eriksen HK, Fantaye Y, Farhang M, Fergusson J, Fernandez-Cobos R, Finelli F, Forastieri F, Frailis M, Fraisse AA, Franceschi E, Frolov A, Galeotta S, Galli S, Ganga K, Génova-Santos RT, Gerbino M, Ghosh T, González-Nuevo J, Górski KM, Grattón S, Gruppuso A, Gudmundsson JE, Hamann J, Handley W, Hansen FK, Herranz D, Hildebrandt SR, Hivon E, Huang Z, Jaffe AH, Jones WC, Karakci A, Keihänen E, Kesikitalo R, Kiiveri K, Kim J, Kisner TS, Knox L, Krachmalnicoff N, Kunz M, Kurki-Suonio H, Lagache G, Lamarre JM, Lasenby A, Lattanzi M, Lawrence CR, Le Jeune M, Lemos P, Lesgourgues J, Levrier F, Lewis A, Liguori M, Lilje PB, Lilley M, Lindholm V, López-Cañiego M, Lubin PM, Ma YZ, Macías-Pérez JF, Maggio G, Maino D, Mandolese N, Mangilli A, Marcos-Caballero A, Maris M, Martin PG, Martinelli M, Martínez-González E, Matarrese S, Mauri N, McEwen JD, Meinhold PR, Melchiorri A, Mennella A, Migliaccio M, Millea M, Mitra S, Miville-Deschênes MA, Molinari D, Montier L, Morgante G, Moss A, Natoli P, Nørgaard-Nielsen HU, Pagano L, Paoletti D, Partridge B, Patanchon G, Peiris HV, Perrotta F, Pettorino V, Piacentini F, Polastri L, Polenta G, Puget JL, Rachen JP, Reinecke M, Remazeilles M,

- Renzi A, Rocha G, Rosset C, Roudier G, Rubiño-Martín JA, Ruiz-Granados B, Salvati L, Sandri M, Savelainen M, Scott D, Shellard EPS, Sirignano C, Sirri G, Spencer LD, Sunyaev R, Suur-Uski AS, Tauber JA, Tavagnacco D, Tenti M, Toffolatti L, Tomasi M, Trombetti T, Valenziano L, Valiviita J, Van Tent B, Vibert L, Vielva P, Villa F, Vittorio N, Wandelt BD, Wehus IK, White M, White SDM, Zacchei A and Zonca A (2020), Sep. Planck 2018 results. VI. Cosmological parameters. *A&A* 641, A6. doi:10.1051/0004-6361/201833910. 1807.06209.
- Pritchard J and Loeb A (2010), Dec. Cosmology: Hydrogen was not ionized abruptly. *Nature* 468 (7325): 772–773. doi:10.1038/468772b.
- Qin Y, Poulin V, Mesinger A, Greig B, Murray S and Park J (2020), Nov. Reionization inference from the CMB optical depth and E-mode polarization power spectra. *MNRAS* 499 (1): 550–558. doi:10.1093/mnras/staa2797. 2006.16828.
- Reichardt CL, Patil S, Ade PAR, Anderson AJ, Austermann JE, Avva JS, Baxter E, Beall JA, Bender AN, Benson BA, Bianchini F, Bleem LE, Carlstrom JE, Chang CL, Chaubal P, Chiang HC, Chou TL, Citron R, Moran CC, Crawford TM, Crites AT, de Haan T, Dobbs MA, Everett W, Gallicchio J, George EM, Gilbert A, Gupta N, Halverson NW, Harrington N, Henning JW, Hilton GC, Holder GP, Holzapfel WL, Hrubes JD, Huang N, Hubmayr J, Irwin KD, Knox L, Lee AT, Li D, Lowitz A, Luong-Van D, McMahon JJ, Mehl J, Meyer SS, Millea M, Mocz LM, Mohr JJ, Montgomery J, Nadolski A, Natoli T, Nibarger JP, Noble G, Novosad V, Omori Y, Padin S, Pryke C, Ruhl JE, Saliwanchik BR, Sayre JT, Schaffer KK, Shirokoff E, Sievers C, Smecher G, Spieler HG, Staniszewski Z, Stark AA, Tucker C, Vanderlinde K, Veach T, Vieira JD, Wang G, Whitehorn N, Williamson R, Wu WLK and Yefremenko V (2021), Feb. An Improved Measurement of the Secondary Cosmic Microwave Background Anisotropies from the SPT-SZ + SPTpol Surveys. *ApJ* 908 (2), 199. doi:10.3847/1538-4357/abd407. 2002.06197.
- Ricotti M (2002), Oct. Did globular clusters reionize the Universe? *MNRAS* 336 (2): L33–L37. doi:10.1046/j.1365-8711.2002.05990.x. astro-ph/0208352.
- Ricotti M and Ostriker JP (2004), Aug. X-ray pre-ionization powered by accretion on the first black holes - I. A model for the WMAP polarization measurement. *MNRAS* 352 (2): 547–562. doi:10.1111/j.1365-2966.2004.07942.x. astro-ph/0311003.
- Rinaldi P, Caputi KI, Iani E, Costantin L, Gillman S, Perez-Gonzalez PG, Ostlin G, Colina L, Greve TR, Noorgard-Nielsen HU, Wright GS, Alvarez-Marquez J, Eckart A, Garcia-Marin M, Hjorth J, Ilbert O, Kendrew S, Labiano A, Le Fevre O, Pye J, Tikkanen T, Walter F, van der Werf P, Ward M, Annunziatella M, Azzollini R, Bik A, Boogaard L, Bosman SEI, Crespo Gomez A, Jermann I, Langeroodi D, Melinder J, Meyer RA, Moutard T, Peissker F, Gudel M, Henning T, Lagage PO, Ray T, Vandenbussche B, Waelkens C and Dayal P (2023), Sep. MIDIS: Unveiling the Role of Strong Ha-emitters during the Epoch of Reionization with JWST. *arXiv e-prints*, arXiv:2309.15671doi:10.48550/arXiv.2309.15671. 2309.15671.
- Robertson BE (2022), Aug. Galaxy Formation and Reionization: Key Unknowns and Expected Breakthroughs by the James Webb Space Telescope. *ARA&A* 60: 121–158. doi:10.1146/annurev-astro-120221-044656. 2110.13160.
- Robertson BE, Ellis RS, Furlanetto SR and Dunlop JS (2015), Apr. Cosmic Reionization and Early Star-forming Galaxies: A Joint Analysis of New Constraints from Planck and the Hubble Space Telescope. *ApJ* 802 (2), L19. doi:10.1088/2041-8205/802/L19. 1502.02024.
- Romano M, Grazian A, Giallongo E, Cristiani S, Fontanot F, Boutsia K, Fiore F and Menci N (2019), Dec. Lyman continuum escape fraction and mean free path of hydrogen ionizing photons for bright $z \sim 4$ QSOs from SDSS DR14. *A&A* 632, A45. doi:10.1051/0004-6361/201935550. 1910.02775.
- Rorai A, Hennawi JF, Oñorbe J, White M, Prochaska JX, Kulkarni G, Walther M, Lukić Z and Lee KG (2017), Apr. Measurement of the small-scale structure of the intergalactic medium using close quasar pairs. *Science* 356 (6336): 418–422. doi:10.1126/science.aaf9346. 1704.08366.
- Santos MG, Ferramacho L, Silva MB, Amblard A and Cooray A (2010), Aug. Fast large volume simulations of the 21-cm signal from the reionization and pre-reionization epochs. *MNRAS* 406 (4): 2421–2432. doi:10.1111/j.1365-2966.2010.16898.x. 0911.2219.
- Schaeffer T, Giri SK and Schneider A (2023), Dec. BEORN: a fast and flexible framework to simulate the epoch of reionization and cosmic dawn. *MNRAS* 526 (2): 2942–2959. doi:10.1093/mnras/stad2937. 2305.15466.
- Sharma M, Theuns T, Frenk C, Bower R, Crain R, Schaller M and Schaye J (2016), May. The brighter galaxies reionized the Universe. *MNRAS* 458 (1): L94–L98. doi:10.1093/mnras/lsw021. 1512.04537.
- Shaw AK, Ghara R, Beniamini P, Zaroubi S and Kumar P (2024), Sep. Asking Fast Radio Bursts (FRBs) for More than Reionization History. *arXiv e-prints*, arXiv:2409.03255doi:10.48550/arXiv.2409.03255. 2409.03255.
- Simmonds C, Tacchella S, Hainline K, Johnson BD, McClymont W, Robertson B, Saxena A, Sun F, Witten C, Baker WM, Bhatawdekar R, Boyett K, Bunker AJ, Charlot S, Curtis-Lake E, Egami E, Eisenstein DJ, Hausen R, Maiolino R, Maseda MV, Scholtz J, Williams CC, Willott C and Witstok J (2024a), Jan. Low-mass bursty galaxies in JADES efficiently produce ionizing photons and could represent the main drivers of reionization. *MNRAS* 527 (3): 6139–6157. doi:10.1093/mnras/stad3605. 2310.01112.
- Simmonds C, Tacchella S, Hainline K, Johnson BD, Puskás D, Robertson B, Baker WM, Bhatawdekar R, Boyett K, Bunker AJ, Cargile PA, Carniani S, Chevallard J, Curti M, Curtis-Lake E, Ji Z, Jones GC, Kumari N, Laseter I, Maiolino R, Maseda MV, Rinaldi P, Stoffers A, Übler H, Villanueva NC, Williams CC, Willott C, Witstok J and Zhu Y (2024b), Sep. Ionising properties of galaxies in JADES for a stellar mass complete sample: resolving the cosmic ionising photon budget crisis at the Epoch of Reionisation. *arXiv e-prints*, arXiv:2409.01286doi:10.48550/arXiv.2409.01286. 2409.01286.
- Singh S, Jishnu NT, Subrahmanyam R, Udaya Shankar N, Girish BS, Raghunathan A, Somashekar R, Srivani KS and Sathyanarayana Rao M (2022), Feb. On the detection of a cosmic dawn signal in the radio background. *Nature Astronomy* 6: 607–617. doi:10.1038/s41550-022-01610-5. 2112.06778.
- Smith BM, Windhorst RA, Cohen SH, Koekemoer AM, Jansen RA, White C, Borthakur S, Hathi N, Jiang L, Rutkowski M, Ryan Russell E. J, Inoue AK, O’Connell RW, MacKenty JW, Conselice CJ and Silk JI (2020), Jul. The Lyman Continuum Escape Fraction of Galaxies and AGN in the GOODS Fields. *ApJ* 897 (1), 41. doi:10.3847/1538-4357/ab8811. 2004.04360.
- Steidel CC, Bogosavljević M, Shapley AE, Reddy NA, Rudie GC, Pettini M, Trainor RF and Strom AL (2018), Dec. The Keck Lyman Continuum Spectroscopic Survey (KLCS): The Emergent Ionizing Spectrum of Galaxies at $z \sim 3$. *ApJ* 869 (2), 123. doi:10.3847/1538-4357/aaed28. 1805.06071.
- Tang M, Stark DP, Topping MW, Mason C and Ellis RS (2024), Aug. JWST/NIRSpec Observations of Ly α Emission in Star Forming Galaxies at $6.5 \lesssim z \lesssim 13$. *arXiv e-prints*, arXiv:2408.01507doi:10.48550/arXiv.2408.01507. 2408.01507.
- Trott CM, Jordan CH, Midgley S, Barry N, Greig B, Pindor B, Cook JH, Slep G, Tingay SJ, Ung D, Hancock P, Williams A, Bowman J, Byrne R, Chokshi A, Hazelton BJ, Hasegawa K, Jacobs D, Joseph RC, Li W, Line JLB, Lynch C, McKinley B, Mitchell DA, Morales MF, Ouchi M, Pober JC, Rahimi M, Takahashi K, Wayth RB, Webster RL, Wilensky M, Wytthe JSB, Yoshiura S, Zhang Z and Zheng Q (2020), April. Deep multiredshift limits on Epoch of Reionization 21 cm power spectra from four seasons of Murchison Widefield Array observations. *MNRAS* 493 (4): 4711–4727. doi:10.1093/mnras/staa414. 2002.02575.
- Verhamme A, Orlitová I, Schaerer D and Hayes M (2015), Jun. Using Lyman- α to detect galaxies that leak Lyman continuum. *A&A* 578, A7. doi:10.1051/0004-6361/201423978. 1404.2958.
- Verhamme A, Orlitová I, Schaerer D, Izotov Y, Worseck G, Thuan TX and Guseva N (2017), Jan. Lyman- α spectral properties of five newly discovered Lyman continuum emitters. *A&A* 597, A13. doi:10.1051/0004-6361/201629264. 1609.03477.
- Walther M, Oñorbe J, Hennawi JF and Lukić Z (2019), Feb. New Constraints on IGM Thermal Evolution from the Ly α Forest Power Spectrum. *ApJ* 872 (1), 13. doi:10.3847/1538-4357/aafad1. 1808.04367.

- Whitler L, Stark DP, Endsley R, Chen Z, Mason C, Topping MW and Charlot S (2024), Apr. Insight from JWST/Near Infrared Camera into galaxy overdensities around bright Lyman-alpha emitters during reionization: implications for ionized bubbles at $z \approx 9$. *MNRAS* 529 (2): 855–872. doi:10.1093/mnras/stae516. 2305.16670.
- Whitler L, Stark DP, Topping MW, Robertson B, Rieke M, Hainline KN, Endsley R, Chen Z, Baker WM, Bhatawdekar R, Bunker AJ, Carniani S, Charlot S, Chevallard J, Curtis-Lake E, Egami E, Eisenstein DJ, Helton JM, Ji Z, Johnson BD, Pérez-González PG, Rinaldi P, Tacchella S, Williams CC, Willmer CNA, Willott C and Witstok J (2025), Jan. The *zrsim9* galaxy UV luminosity function from the JWST Advanced Deep Extragalactic Survey: insights into early galaxy evolution and reionization. *arXiv e-prints*, arXiv:2501.00984doi:10.48550/arXiv.2501.00984. 2501.00984.
- Wilkins SM, Feng Y, Di-Matteo T, Croft R, Stanway ER, Bouwens RJ and Thomas P (2016), May. The Lyman-continuum photon production efficiency in the high-redshift Universe. *MNRAS* 458 (1): L6–L9. doi:10.1093/mnras/slw007. 1512.03214.
- Witstok J, Jakobsen P, Maiolino R, Helton JM, Johnson BD, Robertson BE, Tacchella S, Cameron AJ, Smit R, Bunker AJ, Saxena A, Sun F, Arribas S, Baker WM, Bhatawdekar R, Boyett K, Cargile PA, Carniani S, Charlot S, Chevallard J, Curti M, Curtis-Lake E, D'Eugenio F, Eisenstein DJ, Hainline KN, Jones GC, Kumari N, Maseda MV, Pérez-González PG, Rinaldi P, Scholtz J, Übler H, Williams CC, Willmer CNA, Willott C and Zhu Y (2024a), Aug. Witnessing the onset of Reionisation via Lyman- α emission at redshift 13. *arXiv e-prints*, arXiv:2408.16608doi:10.48550/arXiv.2408.16608. 2408.16608.
- Witstok J, Smit R, Saxena A, Jones GC, Helton JM, Sun F, Maiolino R, Kumari N, Stark DP, Bunker AJ, Arribas S, Baker WM, Bhatawdekar R, Boyett K, Cameron AJ, Carniani S, Charlot S, Chevallard J, Curti M, Curtis-Lake E, Eisenstein DJ, Endsley R, Hainline K, Ji Z, Johnson BD, Looser TJ, Nelson E, Perna M, Rix HW, Robertson BE, Sandles L, Scholtz J, Simmonds C, Tacchella S, Übler H, Williams CC, Willmer CNA and Willott C (2024b), Feb. Inside the bubble: exploring the environments of reionisation-era Lyman- α emitting galaxies with JADES and FRESCO. *A&A* 682, A40. doi:10.1051/0004-6361/202347176. 2306.04627.
- Zackrisson E, Inoue AK and Jensen H (2013), Nov. The Spectral Evolution of the First Galaxies. II. Spectral Signatures of Lyman Continuum Leakage from Galaxies in the Reionization Epoch. *ApJ* 777 (1), 39. doi:10.1088/0004-637X/777/1/39. 1304.6404.
- Zhu Y, Becker GD, Bosman SEI, Keating LC, Christenson HM, Bañados E, Bian F, Davies FB, D'Odorico V, Eilers AC, Fan X, Haehnelt MG, Kulkarni G, Pallottini A, Qin Y, Wang F and Yang J (2021), Dec. Chasing the Tail of Cosmic Reionization with Dark Gap Statistics in the Ly α Forest over $5 < z < 6$. *ApJ* 923 (2), 223. doi:10.3847/1538-4357/ac26c2. 2109.06295.
- Zhu Y, Becker GD, Christenson HM, D'Aloisio A, Bosman SEI, Bakx T, D'Odorico V, Bischetti M, Cain C, Davies FB, Davies RL, Eilers AC, Fan X, Gaikwad P, Haehnelt MG, Keating LC, Kulkarni G, Lai S, Ma HX, Mesinger A, Qin Y, Satyavolu S, Takeuchi TT, Umehata H and Yang J (2023), Oct. Probing Ultralate Reionization: Direct Measurements of the Mean Free Path over $5 < z < 6$. *ApJ* 955 (2), 115. doi:10.3847/1538-4357/accef4. 2308.04614.